The Complementary Relationship in the Estimation of Regional Evapotranspiration: An Enhanced Advection-Aridity Model

by

Michael T. Hobbins, Jorge Ramirez and Thomas C. Brown

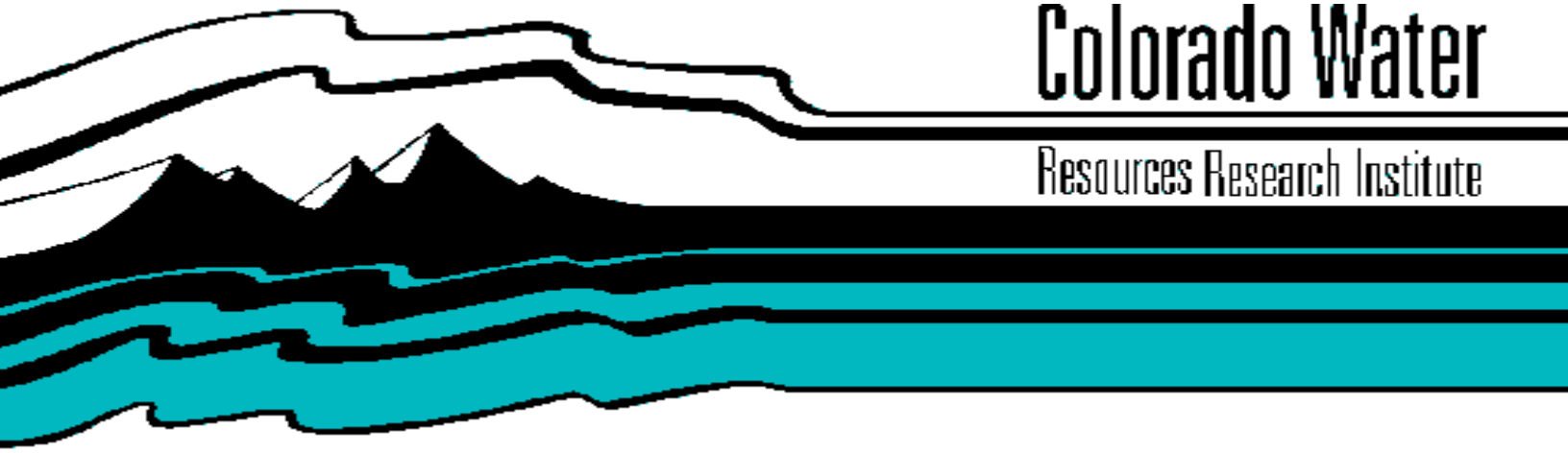

Open File Report No. 13

Colorado State University

OFR 13

THE COMPLEMENTARY RELATIONSHIP IN THE ESTIMATION OF REGIONAL EVAPOTRANSPIRATION: AN ENHANCED ADVECTION-ARIDITY MODEL.

Michael T. Hobbins and Jorge A. Ramírez

Department of Civil Engineering, Colorado State University, Fort Collins, Colorado

Thomas C. Brown

Rocky Mountain Research Station, U.S. Forest Service, Fort Collins, Colorado

ABSTRACT

Results from Brutsaert and Stricker's Advection-aridity evapotranspiration model were compared at the monthly time step with independent estimates of evapotranspiration derived from water balances for 139 large, undisturbed basins across the conterminous U.S. On an average annual basis for the period 1962-1988, the original model, which uses a Penman wind function, underestimated evapotranspiration by 7.9% of precipitation compared with the water-balance estimates. Model accuracy increased with basin humidity. An improved formulation of the model is presented in which the wind function and the Priestley-Taylor coefficient are modified. The wind function was reparameterized on a seasonal, regional basis to replicate independent proxy potential evapotranspiration surfaces. This led to significant differences from the original Penman wind function. The reparameterized wind function, together with a re-calibrated Priestley-Taylor coefficient in the wet environment evapotranspiration formulation, reduced the underestimation of annual average evapotranspiration to only 1.15% of precipitation on an independent set of validation basins. The results offered here lend further support for Bouchet's hypothesis as it applies to large-scale, long-term evapotranspiration.

1. INTRODUCTION

Most evapotranspiration models calculate the drying power of the air as a function of the speed and the vapor pressure deficit of the advected air, but the models often differ in their formulations of the wind function, for which there is currently no standard parameterization [*Brutsaert*, 1982]. The two models examined in *Hobbins et al.* [this issue]—*Morton*'s [1983] Complementary Relationship in Areal Evapotranspiration (CRAE) model and *Brutsaert and Stricker*'s [1979] Advection-aridity (AA) model—exhibit two very different approaches to parameterizing the effects of large-scale advection on regional evapotranspiration (ET_a).

The CRAE model does not use observations of wind speed, but instead calculates potential evapotranspiration using a vapor transfer coefficient f_T, which is dependent on atmospheric pressure but not on wind speed. The AA model relies on the Penman wind function, which was formulated to reproduce point observations of evaporation [*Penman*, 1948]. Of all climatic inputs, the AA model is most sensitive to observed wind speed, whereas the performance of the CRAE model is, to a large extent, independent of wind speed.

As demonstrated in *Hobbins et al.* [this issue], the AA model significantly underestimates ET_a and its performance is highly dependent on basin climatology. To improve this model, it is necessary to examine the advection component of the AA model: the wind function $f(U_r)$ in the potential evapotranspiration (ET_p^{AA}) formulation to remove the

trend, and the Priestley-Taylor coefficient α in the wet environment evaporation (ET_w^{AA}) formulation to remove the bias.

We report here on three methods to reformulate the AA model: the first two attempt to detrend the performance of the model; the last one attempts to remove its bias. First, independent point observations of pan evaporation (ET_{pan}) are used to re-calibrate the wind function on a seasonal basis. Second, a proxy spatially distributed ET_p surface is used to re-calibrate the wind function on a seasonal and regional basis. This proxy ET_p surface is generated by the CRAE model (ET_p^{CRAE}) and used to provide interpolated values for observed ET_{pan} surfaces. Third, once the trend is removed, the Priestley-Taylor coefficient α is optimized such that the errors incurred in closing the water balance have zero mean. The resulting improved AA model yields unbiased, near-zero mean (1.15% of annual precipitation) annual closure errors when validated against independent regional evapotranspiration estimates obtained from long-term, large-scale water balances for undisturbed basins in the conterminous U.S.

2. COMPLEMENTARY RELATIONSHIP

2.1 The hypothesis

The hypothesis of a complementary relationship [*Bouchet*, 1963] states that over areas of a regional scale and away from any sharp environmental discontinuities, there exists a

complementary feedback mechanism between actual and potential evapotranspiration. Energy at the surface that, due to limited water availability, is not taken up in the process of actual evapotranspiration (ET_a) increases the temperature and humidity gradients of the overpassing air, and leads to an increase in ET_p equal in magnitude to the decrease in ET_a. This relationship is described by equation (1):

$$ET_a + ET_p = 2ET_w \quad (1)$$

Under conditions where ET_a equals ET_p, this rate is referred to as the wet environment evapotranspiration (ET_w). Figure 1 illustrates the complementary relationship.

In Section 2.2 , the components of the complementary relationship—ET_p and ET_w—are summarized for the AA model. For a more detailed treatment of this model, see *Hobbins et al.* [this issue] and *Brutsaert and Stricker* [1979]. In this model, ET_p is calculated by combining information from the energy budget and water vapor transfer in the Penman equation, and ET_w is calculated based on derivations of the concept of equilibrium evapotranspiration under conditions of minimal advection, first proposed by *Priestley and Taylor* [1972]. ET_a is then calculated as a residual of (1), constrained such that $ET_a > 0$.

2.2 Advection-aridity model

The AA model calculates ET_p by the Penman equation (2):

$$\lambda ET_p = \frac{\Delta}{\Delta+\gamma} Q_n + \lambda \frac{\gamma}{\Delta+\gamma} E_a \quad (2)$$

where λ represents the latent heat of vaporization, Δ is the slope of the saturated vapor pressure curve at air temperature, γ is the psychrometric constant, and Q_n is the net available energy at the surface. The second term of this combination approach represents the effects of large-scale advection in the mass transfer of water vapor, and takes the form of a scaled factor of an aerodynamic vapor transfer term E_a. E_a, also known as the "drying power of the air," is a product of the vapor pressure deficit (e_a^* - e_a) and a "wind function" of the speed of the advected air $f(U_r)$, of the form (3):

$$E_a = f(U_r)(e_a^* - e_a) \quad (3)$$

In equation (3), U_r represents the wind speed observed at r meters above the evaporating surface, e_a^* and e_a are the saturation vapor pressure and the actual vapor pressure of the air at r meters above the surface, respectively. The wind function $f(U_r)$ is either theoretically or empirically derived. *Brutsaert and Stricker* [1979] suggested the following theoretical expression for the wind function under neutral—i.e., a stable atmospheric boundary layer—conditions:

$$f(U_r) = \frac{\varepsilon a_v k^2 U_r}{R_d T_a \ln[(z_2 - d_0)/z_{0v}] \ln[(z_r - d_0)/z_{om}]} \quad (4)$$

In equation (4), ε is the ratio of the gas constant of dry air R_d to that of water vapor R_v; a_v is the ratio of the eddy diffusivity to the eddy viscosity under neutral conditions; k is the von Karman constant; z_{0m} and z_{0v} are the roughness lengths for momentum and water vapor, respectively; T_a is the air temperature in K; z_2 is the height at which e_a is measured; d_0 is the displacement height; and z_r is the height of the wind measurement.

However, in the context of modeling monthly regional ET_a with the complementary relationship, the effects of atmospheric instability and the onerous data requirements rule out such theoretical formulations. *Penman* [1948] originally suggested the following empirical linear approximation for $f(U_2)$:

$$f(U_2) = 0.26(1 + 0.54U_2) \tag{5}$$

which, for wind speeds at 2 m elevation in m/sec and vapor pressures in mb, yields E_a in mm/day. This formulation of $f(U_2)$ was first proposed [*Brutsaert and Stricker*, 1979] for use in the AA model operating at a temporal scale of a few days. As demonstrated in *Hobbins et al.* [this issue], the AA model increasingly underestimates ET_a with increasing mean annual wind speed, especially for wind speeds above 4 m/sec. This demonstrates the sensitivity of the AA model to the wind function shown above (5) and highlights the need for re-parameterizing this component.

In the agricultural arena, much work has been done to calibrate or reformulate the proposed wind function for use in the combination or Penman equation (e.g., *Allen*

[1986], *Van Bavel* [1966], *Wright* [1982]). These agriculturally oriented formulations operate on a limited spatial and temporal scale, do not hypothesize feedbacks of a regional nature, and require local parameterizations of resistance and canopy roughness. Thus, they are not applicable in predicting regional evapotranspiration.

Substituting the wind function (5) into the Penman equation (2) yields the expression for ET_p (6) used by *Brutsaert and Stricker* [1979] in the original AA model:

$$\lambda ET_p = \frac{\Delta}{\Delta+\gamma} Q_n + \lambda \frac{\gamma}{\Delta+\gamma} 0.26\left(1+0.54U_2\right)\left(e_a^* - e_a\right) \tag{6}$$

In formulating the AA model for use in three-day time-steps, *Brutsaert and Stricker* [1979] ignore any effect of atmospheric stability in the wind function term.

The AA model calculates ET_w [*Brutsaert and Stricker*, 1979] using the *Priestley and Taylor* [1972] partial equilibrium evaporation equation:

$$\lambda ET_w = \alpha \frac{\Delta}{\Delta+\gamma} Q_n \tag{7}$$

where α = 1.28. Support for a re-examination of the Priestley-Taylor coefficient α is provided by work summarized in *Brutsaert* [1982]. An approximate value of α = 1.26 for water surfaces under conditions of minimal advection and in the absence of inversions and condensation from *Priestley and Taylor* [1972] is supported by other researchers: for

well watered grass ($\alpha = 1.27 \pm 0.02$ for perennial ryegrass), *Davis and Allen* [1973]; and for shallow lakes and ponds, and saturated sedge meadow, *Stewart and Rouse* [1976, 1977]. Re-analysis of *Priestley and Taylor*'s [1972] results suggests $\alpha = 1.28$. Other, more significant variations are also reported: e.g., $\alpha = 1.05$ for short, well watered Douglas Fir [*McNaughton and Black*, 1973]. Work on a shallow lake [*DeBruin and Keijman*, 1979] found intra-daily variations in α ranging from 1.15 early in the day to 1.42 in the afternoon, and seasonal variations ranging from 1.20 for August to 1.50 for April.

Morton [1983] suggests that $\alpha = 1.32$ be used instead of $\alpha = 1.26$ or 1.28, as the latter values were derived from averages across free water and land surfaces [*Priestley and Taylor*, 1972] and probably underestimate the value for land surfaces alone, due to their greater roughness and heterogeneity. *Morton* [1983] also refutes the assumption of no limitations on the availability of water for evapotranspiration.

Potential evapotranspiration surfaces from the CRAE model, described in *Hobbins et al.* [this issue], are used in this study as proxy ET_p surfaces. As in the AA model, ET_p^{CRAE} is calculated by combining information from the energy budget and water vapor transfer. However, the CRAE model relies on the concept of an equilibrium temperature between the surface and the over-passing air and a wind speed-independent vapor transfer function to compute ET_p.

3. METHODOLOGY

3.1 Model Performance

This section briefly lists the data sets and equations used in the generation of the estimates of evapotranspiration, describes the long-term, large-scale water balances and the data sets from which the input variables (streamflow and precipitation) were obtained, and describes the mean annual water balance closure errors. For more detail, see *Hobbins et al.* [this issue].

To generate the model estimates of evapotranspiration ET_a^{MODEL}, the following data sets were used:

- Temperature: "NCDC Summary of the Day" [*EarthInfo*, 1998a].

- Wind speed: "Solar and Meteorological Surface Observation Network (SAMSON) " [*NREL*, 1992] and "U.S. Environmental Protection Agency Support Center for Regulatory Air Models (EPA SCRAM)."

- Solar Radiation: "Solar and Meteorological Surface Observation Network (SAMSON)" [*NREL*, 1992].

- Humidity: "NCDC Surface Airways" [*EarthInfo*, 1998b].

- Albedo: an update from the *Gutman* [1988] average monthly albedo surfaces (G. Gutman, personal communication, 1995).

- Elevation: a 30-arc second DEM (NOAA-NGDC).

In order to generate areal evapotranspiration coverages, spatial interpolation techniques were applied to the point observations of the input variables. All spatial interpolation and analyses were conducted at a 10km cell size for the conterminous United States for a period of study (water years 1962-1988).

Assuming stationary conditions for the climatic forcing, the long-term (i.e., climatological), large-scale water balance for an undisturbed basin should lead to negligible net changes in overall basin moisture storage. For a control volume including the ground surface and transpiring canopy and extending to the groundwater aquifer, the long-term, steady state, water balance can be expressed as:

$$ET_a^* = P - Y \tag{12}$$

In equation (12), P represents basin-wide precipitation and Y represents basin yield, both expressed as depth equivalents. Y includes contributions from both surface and groundwater flow and, in the manner of *Eagleson* [1978], is estimated by the observed streamflow. Thus, an estimate of the long-term average annual evapotranspiration ET_a*

can be obtained from independent data on precipitation and streamflow, for which the following datasets were used:

- Streamflow: "A Daily Hydroclimatological Data Set for the Continental United States" [*Wallis et al.*, 1991] and the U.S. Geological Survey (USGS) "Hydro-Climatic Data Network (HCDN)" [*Slack and Landwehr*, 1992].

- Precipitation: "Parameter-elevation Regressions on Independent Slopes Model (PRISM)" [*Daly et al.*, 1994].

This estimate, henceforth referred to as the "independent evapotranspiration estimate" or ET_a*, can be compared with the long-term average annual value obtained from monthly evapotranspiration estimates using the complementary relationship models, and provides a means to verify the models.

Basins of minimal anthropogenic impact were selected for the long-term analysis of the water balance components from among those basins included in the two streamflow data sets listed above. Only basins whose digital USGS 8-digit Hydrologic Unit Code (HUC) boundaries closely matched (+/- 15%) the areas for the corresponding gauges were used. This resulted in a set of 139 basins, which contain a total of 351 HUCs and constitute 17.4% of the conterminous United States. Table 1 classifies the selected basins by size.

The measure of the performance of the model—the "average annual water balance closure error," or "closure error"—is derived by comparing the model evapotranspiration ET_a^{MODEL} to the independent evapotranspiration estimate ET_a^*. The closure error for each model $\varepsilon^{\text{MODEL}}$ is calculated for each basin, as a percentage of average annual precipitation, from equation (13):

$$\varepsilon^{MODEL} = \frac{\sum_{i=1}^{27}\sum_{j=1}^{12}\left(ET^{*}_{a_{(i,j)}} - ET^{MODEL}_{a_{(i,j)}}\right)}{\sum_{i=1}^{27}\sum_{j=1}^{12}P_{(i,j)}} * 100\% \qquad (13)$$

where ET_a^{MODEL} is the model estimate of ET_a (i.e., ET_a^{AA} or ET_a^{CRAE}), and i and j are the water year and month, respectively.

Non-zero closure errors must first be considered to be either an over-prediction (negative closure error) or under-prediction (positive closure error) of evapotranspiration by the models. Other possible explanations—not quantified in this study—are: (i) violations of the assumptions inherent in equation (12), perhaps through the effects of groundwater pumping, surface-water diversions, or violations of the assumption of negligible net groundwater flow out of the basin; (ii) violations of the assumption of stationarity in climatological forcing; (iii) errors in the hydroclimatological record; and (iv) errors induced by spatial interpolation of the climatic variables.

3.2 ET_p reparameterization

Combining equations (2) and (3) yields the following expression for back-calculating the wind function $f(U_2)$:

$$f(U_2) = \left(ET_p^{\,INDEP} - \frac{\Delta}{\Delta+\gamma}\frac{Q_n}{\lambda} \right) \frac{\Delta+\gamma}{\gamma\left(e_a^* - e_a\right)} \tag{14}$$

In the following two sections, methods for estimating a new regional, seasonal wind function are described. The first uses point observations of pan evaporation ET_{pan} as an independent measure of potential evaporation ET_p^{INDEP}. The second uses ET_p^{CRAE} as a proxy for ET_p^{INDEP}. Both methods back-calculate values for $f(U_2)$, which are compared to observations of U_2 to create the necessary U_2-$f(U_2)$ relationships. The AA model is then reformulated to reflect the new $f(U_2)$ relationships, creating the AA(1) model from the ET_{pan} calibration and the AA(2) model from the ET_p^{CRAE} calibration.

3.2.1 Estimates of ET_p^{INDEP} using ET_{pan} observations

At a point in a homogeneous region of scale lengths on the order of 1-10 km, the complementary relationship indicates that a free-water surface will evaporate at the potential rate ET_p. Thus, if the aerological conditions are known (i.e., temperature, humidity, and solar radiation), pan evaporation (ET_{pan}) observations can be used on a seasonal (i.e., monthly) basis to back-calculate the value of the drying power of the air E_a, and hence, the value of the wind function $f(U_2)$, using equation (14), with ET_{pan} substituted for ET_p^{INDEP}. The values of $f(U_2)$ are then combined with the observed wind

speeds at the station to generate the empirical monthly relationships between U_2 and $f(U_2)$, $(U_2\text{-}f(U_2))$.

Monthly pan evaporation (ET_{pan}) data are drawn from 14 stations across the conterminous United States in the data set "NCDC Summary of the Day" [*EarthInfo*, 1998a]. These stations are then matched to the closest (i.e., within 1 minute Lat/Long) reporting SAMSON stations [*NREL*, 1993], from which the other climatological input data (average temperature, solar radiation, and humidity) are drawn.

The resulting $f(U_2)$ values are then compared, on a monthly basis, to the wind speeds observed at the SAMSON stations. For each month, a least-squares fit is derived to express this relationship. The AA model is re-coded to reflect the seasonal $f(U_2)$ expressions, creating the AA(1) model, and the water balance closure errors ($\varepsilon^{AA(1)}$) are recalculated.

3.2.2 Estimates of ET_p^{INDEP} using ET_p^{CRAE}

The spatial patterns and values of the average annual ET_p^{CRAE} surface (Figure 2b, *Hobbins et al.* [this issue]) closely match the contours of the climatological (1931-1960) surface of pan evaporation derived from spatially interpolated observations [*USGS*, 1970]. Thus, in the absence of any other source of independent and spatially distributed ET_p data, the monthly ET_p^{CRAE} surfaces are used as proxy ET_{pan} data. The Penman wind function in the AA model $f(U_2)$ is then calibrated to the proxy ET_{pan} data.

Given that monthly ET_p^{CRAE} data are available over the entire study area, it was possible to derive monthly wind functions that applied for each region of the study area. To this end, the study area (i.e., the conterminous United States) was divided into the 18 management regions defined by the USGS water resource regions (WRR). Two-thirds of the original set of 139 basins were selected for a calibration subset, leaving the remaining one-third for a validation subset. For the calibration subset, only basins containing a single HUC or a combination of two HUCs were selected, with each HUC appearing in one basin, at most. This resulted in a calibration subset of 92 basins containing 110 HUCs, covering an area of 394 x 10^3 km^2, or 4.9% of the conterminous United States.

Substituting spatially integrated ET_p^{CRAE} values for ET_p^{INDEP} in equation (14), and using monthly basin-wide depths for ET_p^{CRAE}, Q_n, and monthly spatial averages for Δ, γ, ($e_a^* - e_a$), and U_2, values of $f(U_2)$ were back-calculated for each month and each basin in the calibration subset in each WRR. Basin-months for which constraints applied (i.e., months where $\min(Q_n) < 0$, $\min(e_a^* - e_a) < 0$, $\min(ET_w) < 0$) were excluded. This resulted in 26040 values of $f(U_2)$ and U_2 spread between the 216 WRR-month combinations (i.e., 18 WRRs and 12 months).

In order to generate new regional, seasonal (monthly) wind functions, least squares linear regressions were conducted on the U_2- $f(U_2)$ relationship on a monthly and regional basis. Months that did not have sufficient data (i.e., fewer than an arbitrarily chosen 27 values) were infilled from surrounding months. One WRR (i.e., 16) did not have any data as

there were no basins selected in this WRR. The regression for this WRR involved stations from surrounding WRRs (i.e., WRRs 10, 14, 15, 17, and 18), on the basis of their being the closest to the WRR in question.

Again, to test the performance of the new, regional and seasonal wind function in the long-term, large-scale water balances, the AA model was reformulated to reflect these new regional, seasonal $f(U_2)$-U_2 relationships, creating the AA(2) model. The water balance closure errors ($\varepsilon^{AA(2)}$) were recalculated for the full set of 139 basins following the procedures previously outlined.

3.3 ET_w recalibration

With ET_p^{AA} formulated to be independent of advection, attention must turn to removal of the positive bias in the AA(2) water balance closure errors. This bias results from the underestimation of ET_a, and may be removed by increasing the Priestley-Taylor coefficient α in equation (7). This would have the effect of increasing ET_w, and hence ET_a.

For the calibration set of 92 basins previously described, monthly surfaces of ET_w were generated for a range of α values in order to isolate the α yielding a zero mean annual closure error ε^{AA}. Note that the regional, seasonal wind functions $f(U_2)$ in the ET_p formulation described in Section 3.2.2 were used in conjunction with each trial ET_w run. This recalibration results in the AA(2*) model.

4. RESULTS

Figures 2a and 2b summarize results from work reported in *Hobbins et al.* [this issue] on the original CRAE and AA models. Figure 2a presents the empirical distribution of the complete set of 139 closure errors for both models. Summary statistics are listed in Table 2. The ranges are approximately +25% to –20% for the CRAE model, with one low outlier below –30%, and +35% to –15% for the AA model, with five outliers. Neither model yields closure errors that are normally distributed.

Figure 2b shows the relationship between ε^{MODEL} and mean annual basin wind speed. The CRAE results are included here to demonstrate the effects of its different advection formulation. The ε^{AA} are strongly positively correlated with—and hence the AA model is very sensitive to—wind speed (slope = 0.1152, $R^2 = 0.36$, $p < 0.05$). The ε^{CRAE} are weakly negatively correlated with wind speed ($R^2 = 0.04$, $p < 0.05$). They are clustered around zero for the lowest wind speeds and increase in variability with increasing wind speed. This near-independence of the CRAE model's performance with wind speed appears to support *Morton*'s [1983] treatment of advection.

4.1 Reparameterization of ET_p^{AA} using ET_{pan}

Figure 3 shows an example (August) of the monthly $f(U_2)$-U_2 relationship derived by substituting point observations of ET_{pan} for ET_p^{INDEP} in equation (14). The least-squares linear fit to the observed $f(U_2)$-U_2 relationship yields the following equation (15) for the August wind function:

$$f(U_2) = 0.4703U_2 - 0.1954, \qquad R^2 = 0.47, \qquad p < 0.05 \tag{15}$$

Graphically, the least squares linear fit for the observed $f(U_2)$-U_2 relationship, expressed in equation (15), is steeper and higher across the observed U_2 range than that predicted by the Penman wind function, expressed in equation (5), used in the *Brutsaert and Stricker* [1979] AA model. The estimate for $f(U_2)$ for August from equation (15) is then higher than that of the Penman wind function in equation (5), which, when compared to the AA model, leads to a higher estimate of ET_p and, thereby, a lower estimate of ET_a. This is, in fact, the case for all months in the growing season (May through September). For the rest of the year, the magnitude of the observed $f(U_2)$-U_2 relationship is approximately equal to that of (5), although often slightly offset. Given that annual evapotranspiration totals are highly skewed towards warmer months, these differences should lead to increasingly positive water balance closure errors across the study basins when compared to the AA model.

Figure 4a indicates that this is indeed the case for the complete set of basins. The histogram of closure errors for the AA(1) model has shifted to the right, indicating that it is predicting a lower ET_a than the AA model. Although the skewness has increased from

–1.7501 for the ε^{AA} to 0.5117 for the $\varepsilon^{AA(1)}$, reflecting a more normal distribution with a preponderance of positive values, the null hypothesis of normality must still be rejected. The mean closure error has increased from 7.92% to 27.05%. The maximum and minimum also indicate this shift: from 30.11% to 74.21% and –48.71% to –16.47%, respectively. The standard deviation also compares poorly: increasing from 12.67% to 18.98%.

Figure 4b shows the water balance closure errors $\varepsilon^{AA(1)}$ plotted against mean annual wind speed. Included for comparison is the relationship already established [*Penman*, 1948; *Brutsaert and Stricker*, 1979] for the AA model. The most striking feature of this plot is that the closure errors for the AA(1) model show a stronger relationship to wind speed than do those of the AA model. Below about 4 m/sec, the $\varepsilon^{AA(1)}$ appear to be independent of wind speed. However, above 4 m/sec, the $\varepsilon^{AA(1)}$ are strongly correlated with wind speed. Thus, for a given wind speed, the AA(1) model tends to over-estimate ET_p and hence under-estimate ET_a to an even greater degree than the original AA model.

As this reformulation of the Penman wind function did not improve the performance of the AA model with respect to advection, no further work was performed.

4.2 Reparameterization of ET_p^{AA} using ET_p^{CRAE}

The general effects of the ET_p^{CRAE}-based reparameterization are illustrated in the results for WRR 11 (Arkansas-White-Red Region). Figure 5a shows the monthly $f(U_2)$-U_2

relationships derived by substituting for ET_p^{INDEP} in equation (14) the 1150 monthly basinwide totals of ET_p^{CRAE} from the five calibration basins in WRR 11. The solid lines represent the least-squares linear fit of these relationships; the dashed lines represent the original, non-seasonal Penman wind function used in the *Brutsaert and Stricker* [1979] AA model, expressed mathematically in equation (5). There are two prominent findings from these plots.

First, for all months, the slope of the relationship between U_2 and $f(U_2)$ is less than that predicted by the Penman wind function in equation (5). This indicates that the effects of increasing wind speeds on the value of ET_p are less pronounced than for the Penman wind function used in the AA model. From March to September, the relationship between U_2 and $f(U_2)$ is still positive, in common with empirical wind functions in general. From October to February, however, the relationship is negative. Within these months, applying the derived regional, seasonal wind functions would lead to lower estimates of ET_p for higher values of U_2 and vice-versa. This is contrary to the Penman wind function (5), which predicts increasing $f(U_2)$, and hence increasing ET_p^{AA}, for increasing U_2.

In general, of the total of 197 directly observed (i.e., not filled in from surrounding data) $f(U_2)$-U_2 relationships derived for all months and regions, only one has a slope more positive than the Penman wind function (5). In fact, 111 of the slopes of observed $f(U_2)$-U_2 relationships are negative.

Second, the data for November through June lie predominantly below the line predicted by the Penman wind function (5), leading to lower estimates of ET_p^{AA} than those predicted by the Penman wind function. This, in turn, would lead to increasing estimates of ET_a^{AA}. The data for the other months, July through September, lie approximately on the Penman line. Thus, for a given wind speed during these summer months, the AA(2) model would predict similar values to those of the AA model, dependent on the wind speed. Given that slopes of the $f(U_2)$-U_2 relationships in these months are lower than the Penman, one would expect, when compared to the AA model, to see higher estimates of ET_p for lower wind speeds and vice-versa. It should be noted, however, that the months with the positive slopes, as predicted by other empirical $f(U_2)$ formulations, are those months with the highest R^2 values for the regressed relationship (between 0.39 and 0.65).

Evapotranspiration totals in the annual cycle are highly skewed towards warmer months (July through October), for which the $f(U_2)$-U_2 relationships established using the AA(2) model are similar to, but at a lower slope than, the Penman wind function in equation (5). The combined effects of these differences and those of the remaining months (November through June), for which the derived relationships are both lower and at a lower slope than the Penman wind function in equation (5), upon the long-term, large-scale water balances would be difficult to predict. The mean monthly values of wind speed for the basins in WRR 11 are the lowest for the warmest months, and in fact lie in the regions of the relationships established for these months that are to the left of the Penman line. Hence, in general, higher ET_p estimates and correspondingly lower ET_a estimates should be expected for these months. Three of the five closure errors of the calibration basins in

WRR 11 increase from the AA model to the AA(2) model (from 4.25% to 5.83%, 5.84% to 6.52%, and 10.88% to 11.20%). The other two decrease (from 18.00% to 0.71% and 28.16% to 18.43%). Of the two validation basins in WRR 11, one closure error decreases (from 23.73% to 7.38%) while the other increases (from 2.60% to 3.66%). The fact that the effect of this reparameterization on the closure errors for the basins in WRR 11 is so mixed indicates that, to varying degrees, the underestimation in ET_a engendered in the calmer summer months is mitigated by the overestimation in the other, windier months.

In general, the combination of the changes in ET_p^{AA} (i.e., the lower slopes and values of the observed relationships when compared with the Penman wind function (5)) wrought by the regional, seasonal $f(U_2)$-U_2 relationships should therefore be to decrease the monthly ET_a^{AA} estimates for basin-months with high wind speeds while—especially from November to June—having little effect on basin-months with lower wind speeds. This should have the effect of reducing the apparent dependence of the closure errors upon wind speed observed in Figure 2b.

Figure 5b displays the empirical frequency distributions of closure errors for the validation, calibration and combined (complete) basin sets in the AA(2) model and the original AA model. For the validation basin set, the distribution of $\varepsilon^{AA(2)}$ appears to be more normal than that of ε^{AA}, as reflected in the reduction of the skewness from –1.6571 for ε^{AA} to –1.0156 for $\varepsilon^{AA(2)}$. However, the null hypothesis of normality must still be rejected at the 95% significance level. For the validation set of basins, the mean has decreased: +8.56% for ε^{AA} to +7.93% for $\varepsilon^{AA(2)}$, and the standard deviation has

decreased: 13.45% for ε^{AA} to 5.32% for $\varepsilon^{AA(2)}$. In applying the AA(2) model, of the five outliers—defined as ε^{MODEL} values below -30%—four have significantly improved ET_a estimates (closure errors have gone from -38.31% to –7.10%, –33.34% to –16.59%, –37.42% to –14.45%, and –34.69% to +6.58%), while the fifth has improved from ε^{AA} = -48.71 to $\varepsilon^{AA(2)}$ = -37.79%. These outliers are discussed at some length in *Hobbins et al.* [this issue]. Summary statistics for both models are presented in Table 2.

Figure 5c shows the $\varepsilon^{AA(2)}$ sets plotted against mean annual basinwide wind speed. The relationship of $\varepsilon^{AA(2)}$ with respect to wind speed derived as a result of this parameterization appears to be independent of mean annual wind speed. As regards the validation basin set, the least-squares linear fit is horizontal (slope = 0.028 (%/msec^{-1}), R^2 = 0.14, $p < 0.05$). Included for comparison in Figure 5c is the linear relationship established for the original AA model complete basin set.

Although the relation of wind speed to closure error appears to have been removed in the AA(2) model, the consistent underestimation may be best addressed by recalibrating a component of the complementary relationship that is independent of wind speed, namely the ET_w^{AA} component.

4.3 ET_w recalibration

Figure 6 shows the AA(2) mean closure errors of the calibration set for each trial value of α. The relationship between water balance closure error and α yields a zero mean closure

error at α = 1.3177. Although equations (1), (7), and (13) suggest that this relationship should be approximately linear, that the relationship is so linear is surprising given the constraints on the values of the components of the complementary relationship, all of which have the effect of rendering this relationship non-linear. Note that the standard deviation of the calibration set of closure errors increases with increasing α, and moves from $\sigma(\varepsilon^{AA})$ = 9.25% for the original value of α = 1.28 to $\sigma(\varepsilon^{AA})$ = 10.51% for the recalibrated value of α = 1.3177.

Figure 7a shows a histogram of the complete set of AA(2*) closure errors resulting from using the value of α of 1.3177, i.e., the value that minimizes the mean closure error, and the seasonally, regionally re-parameterized wind function. Table 2 includes the summary statistics for this run, for the calibration run , and for the complete set of basins.

In adapting the AA(2) model to the AA(2*) model, which uses the optimized value of α = 1.3177 in its ET_w formulation, the main effect has been to shift the distribution to the left. This leads to an improvement in model performance, which is reflected in the summary statistics for the validation sets of both the AA(2) and the AA(2*) runs. In progressing from the AA(2) model to the AA(2*) model, the median closure error of the validation set has decreased from 8.21% to 1.65%, and the mean has decreased from 7.93% to 1.15%. The standard deviation for the validation set has increased from 5.32% to 6.66%, but there is little change in the skewness, from -1.0156 to -1.0886, with the null hypothesis of normality rejected for both validation sets. For the complete set of basins,

the AA(2*) model (skewness = -1.6049) still represents an improvement over the original AA model (skewness = -1.7501) as far as normality is concerned.

Figures 7b through 7d display the effects of basin climatology on the performance of the AA(2*) model. Included on these figures are the least squares linear fits to the $\varepsilon^{AA(2*)}$ results for the validation, calibration and complete basin sets. Also shown are the linear fits for the complete set of closure errors ε^{AA} for the original AA model. The ε^{AA} data themselves are displayed in *Hobbins et al.* [this issue] (see Figures 8a (precipitation), 8b (ET_a*), and 10 (wind speed)). The regression analyses described below refer to the complete basin set.

As expected, the results for wind speed (Figure 7b) indicate a significant improvement over the original AA model (slope = 0.1152, $R^2 = 0.36$, $p < 0.05$). The least squares linear fit lies almost directly along the $\varepsilon^{AA(2*)} = 0$ (slope = $9.73*10^{-4}$, $R^2 = 4.7*10^{-5}$, $p = 0.09359$), indicating that the wind speed dependence evident in the original AA model has been eliminated. Also, the positive bias (i.e., towards underestimation of ET_a) evident in the results for the original AA model and the AA(2) model (see Figure 5c) has been completely removed.

Regression analysis on the precipitation data (Figure 7c) indicates that, while there is no significant relationship (slope = $-3.7*10^{-5}$, $R^2 = 0.01$, $p = 0.22$) between precipitation and ε^{AA}, the $\varepsilon^{AA(2*)}$ increase very slightly (slope = $8.45*10^{-5}$, $R^2 = 0.11$, $p < 0.05$) with precipitation. The R^2 value indicates that the $\varepsilon^{AA(2*)}$ stick close to this relationship; also

there is no bias, as previously discussed. The AA(2*) model tends to overestimate ET_a* for basins with less than 700 mm/year of precipitation, and underestimate for basins over 700 mm/yr. A basin at 3100 mm/year is not shown, although it is included in the analysis of the calibration and complete sets.

Although the slope of the relationship between ET_a* and $\varepsilon^{AA(2*)}$ (Figure 7d) indicates a stronger positive relationship (slope = $2.2*10^{-4}$, $R^2 = 0.14$, $p < 0.05$) than between ET_a* and ε^{AA}, the R^2 value indicates that the $\varepsilon^{AA(2*)}$ adhere to the regressed relationship more closely than in the case of the AA model (slope = $5.38*10^{-5}$, $R^2 = 4.4*10^{-3}$, $p = 0.44$). Also, the slope of the regressed relationship for the ε^{AA}, although nominally flatter, is not statistically significant at the 95% level. This is borne out by examining Figure 7b in *Hobbins et al.* [this issue].

5. SUMMARY AND CONCLUSIONS

The objectives of this study were to examine the Advection-Aridity model of the hypothesis of a complementary relationship between actual and potential regional evapotranspiration with respect to its treatment of advection, and to attempt to improve the model. Evaluation proceeded by comparing evapotranspiration estimates produced by the original AA model with independent estimates obtained from long-term, large-scale water balances. Improvements to the model took the form of including a monthly, regionally reparameterized wind function in the ET_p formulation to remove wind speed

dependence, and recalibrating the Priestley-Taylor coefficient α in the ET_w formulation to remove the bias towards underestimation of ET_a.

As shown in Table 2, the original AA model presented by *Brutsaert and Stricker* [1979] performed poorly, generating—for the complete set of 139 basins—an average annual closure error of –7.92% and a standard deviation of 12.67%. With the exception of a few outliers, which are discussed in *Hobbins et al.* [this issue], the general trend is towards positive AA closure errors. This may result from a poorly calibrated wind function.

The AA model's performance is affected by basin climatology, generally underestimating ET_a in all but the most arid climates. Scatterplots of closure error versus aridity measures (Figures 8a, 8b, and 8c in *Hobbins et al.* [this issue]) show that ε^{AA} increase in variability with increasing aridity but converge towards zero with increasing humidity.

These results indicate that the predictive powers of the AA model increase in moving towards regions of increased climate control of evapotranspiration rates and decrease in moving towards regions of increased soil control. Increased climate/soil control in this context refers to increased and decreased moisture availability respectively. Since irrigated agriculture is often associated with areas of low moisture availability, these trends could be a direct reflection of anthropogenic influences, i.e., through net groundwater withdrawals and net diversion of surface waters.

The CRAE model performed considerably better than did the original AA model [*Hobbins et al.,* this issue]. One of the primary differences between the original AA model and the CRAE model is in their treatments of advection. The AA model uses actual wind speed data to calculate the drying power of the air E_a in the expression for ET_p^{AA}, whereas the CRAE model calculates ET_p^{CRAE} by use of a vapor transfer coefficient f_T and does not use observations of wind speed. The relatively low mean annual CRAE closure error appears to support *Morton*'s [1983] reasoning for his parameterization of the wind function. However, the negative correlation observed between the CRAE closure errors and climatological basin-wide wind speed—although weak—suggests that there is some opportunity to improve this model's treatment of advection. The strong correlation of the AA closure errors with wind speed clearly demonstrates the sensitivity of this model to the wind function $f(U_2)$, first proposed [*Brutsaert and Stricker*, 1979] for use in the AA model operating at a temporal scale of the order of days, and highlights the need for a reparameterization of this component of ET_p^{AA} to yield both accurate ET_p estimates and unbiased water balance estimates on a monthly basis.

Although the use of ET_{pan} data to derive seasonal wind functions represents an independent means of reparameterizing the ET_p component of the AA model, as presented it does not produce any improvement in the model's treatment of advection. In fact, the modified model AA(1) performs significantly worse than the original AA model with the original Penman wind function. This is most likely due to experimental procedure. The stations recording the ET_{pan} may have been too far removed from the

stations recording the aerological conditions. Many stations over much of the study area do not record ET_{pan} data outside of the growing season, leading to a paucity of data and a spatial bias in the ET_{pan} data used for these periods. The assumption that the data from the SAMSON stations accurately represent aerological conditions over homogenous areas large enough for the complementary relationship to hold is weak and easily violated.

Using the ET_p^{CRAE} surfaces as proxy independent ET_p estimates and thereby replacing the original Penman wind function (5) with a regionally recalibrated, seasonal wind function yielded much-improved results. The dependence of the closure errors on wind speed in the original AA model was removed in the AA(2) model, the mean of the validation set of basins was reduced from 8.56% to 7.93%, and the standard deviation was reduced from 13.45% to 5.32%.

Removal of the positive bias in the closure errors entailed optimizing the Priestley-Taylor coefficient α subject to the constraint of a minimum mean closure error for a calibration subset of 92 basins. This procedure yielded a value of $\alpha = 1.3177$, very close to the value ($\alpha = 1.32$) predicted by *Morton* [1983] in his re-assessment of results reported by *Priestley and Taylor* [1972]. Use of $\alpha = 1.3177$ with the regional, seasonal wind function further reduced the mean closure error of the validation set to 1.15%, and of the complete set of 139 basins to 0.39%. The standard deviation of the closure errors increased slightly to 6.66% for the validation set and 9.37% for the complete set, which still represents a significant improvement over 13.45% for the validation set and 12.67% for the complete set for the original *Brutsaert and Stricker* [1979] model.

The low mean annual water balance closure errors for the CRAE model (see *Hobbins et al.* [this issue]) and the improved seasonal, regional AA(2*) model offered here indicate the utility of models based on the hypothesis of a complementary relationship in regional evapotranspiration for providing independent estimates of ET_a. For homogenous areas at regional scales, these complementary relationship models are preferred over traditional evapotranspiration models using land-based parameterizations, as they explicitly account for the soil moisture dependence of potential evapotranspiration, their data requirements are significantly lighter, and they require no local calibration of parameters.

This paper outlines procedures that enable re-parameterization of the model for application in other regions. Research continues into the behavior of these models in mountainous and high-elevation basins.

ACKNOWLEDGMENTS

This work was partially supported by the Strategic Planning and Resource Assessment of the US Forest Service and the US Department of Energy National Institute for Global Environmental Change. In addition, one of the co-authors (Jorge A. Ramírez) received partial support from the Colorado Water Resources Research Institute.

REFERENCES

Allen, R. G. A Penman for all seasons. *J. Irrig. and Drain. Eng.*, 112(4): 348-368, 1986.

Ben-Asher, J. Estimating evapotranspiration from the Sonoita Creek watershed near Patagonia, Arizona. *Water Resour. Res.*, 17(4): 901-906, 1981.

Bouchet, R. J. Evapotranspiration réelle evapotranspiration potentielle, signification climatique. Int. Assoc. Sci. Hydrol., Proceedings, Berkeley, Calif., Symp. Publ. 62: 134-142, 1963.

Bras, R. L., and I. Rodríguez-Iturbe. *Random Functions and Hydrology*, 559 pp., Dover, NY, 1993.

Brutsaert, W., and H. Stricker. An advection-aridity approach to estimate actual regional evapotranspiration. *Water Resour. Res.*, 15(2): 443-450, 1979.

Brutsaert, W. *Evaporation into the Atmosphere: Theory, History, and Applications*, 299 pp., D Riedel, MA, 1982.

Calder, I. R. What are the limits on forest evporation? – A further comment. *J. Hydrol.* 89: 33-36, 1986.

Chiew, F. H. S., and T. A. McMahon. The applicability of Morton's and Penman's evapotranspiration estimates in rainfall-runoff modeling. *Water Resour. Bul.*, 27(4): 611-620, 1991.

Claessens, L. The complementary relationship in regional evapotranspiration and long-term large-scale water budgets, MS thesis, Hydrologic Science and Engineering Program, Civil Engineering Department, Colorado State University, Fort Collins, Colorado, U.S.A., 159 pp., 1996.

Daly, C., R. P. Neilson, and D. L. Phillips. A statistical-topographic model for mapping climatological precipitation over mountainous terrain, *Journal of Applied Meteorology*, 33(2): 140-158, 1994.

Davenport, D.C., and J. P. Hudson. Local advection over crops and fallow. I. Changes in evaporation along a 17-km transect in the Sudan Gezira. *Agricultural Meteorology*, 4: 339-352, 1967.

Dolph, J., and D. Marks. Characterizing the distribution of observed precipitation and runoff over the continental United States. *Climatic Change*, 22: 99-119, 1992.

Dooge, J. C. I. Hydrologic Models and Climate Change. *J. of Geophys. Res.*, 97(D3): 2677-2686, 1992.

Doyle, P. Modeling catchment evaporation: An objective comparison of the Penman and Morton approaches. *J. Hydrol.*, 12: 257-276, 1990.

Eagleson, P. S. Climate, soil and vegetation: 7. A derived distribution of annual water yield, *Water Resources Research*, 14(5): 765-776, 1978.

Eichinger, W. E., M. B. Parlange, and H. Stricker. On the concept of equilibrium evaporation and the value of the Priestley-Taylor coefficient. *Water Resour. Res.*, 32(1) 161-164, 1996.

Granger, R. J. A complementary relationship approach for evaporation from nonsaturated surfaces. *J. Hydrol.*, 111: 31-38, 1989.

Granger, R. J., and D. M. Gray. Examination of Morton's CRAE model for estimating daily evaporation from field-sized areas. *J. Hydrol.*, 120: 309-325, 1990.

Gutman, G. A simple method for estimating monthly mean albedo from AVHRR data. *Journal of Applied Meteorology, 27(9)*: 973-988, 1988.

Hobbins, M. T., J. A. Ramírez, and T. C. Brown. The complementary relationship in regional evapotranspiration : the CRAE model and the Advection-aridity approach. *Proc. Nineteenth Annual A.G.U. Hydrology Days*: 199-212, 1999.

Hobbins, M. T., J. A. Ramírez, T. C. Brown, and L. H. J. M. Claessens. The complementary relationship in the estimation of regional evapotranspiration: the CRAE and advection-aridity models. *Water Resour. Res.*, this issue.

Kim, C. P., and D. Entekhabi. Examination of two methods for estimating regional evaporation using a coupled mixed layer and land surface model. *Water Resour. Res.*, 33(9): 2109-2116, 1997.

Kitanidis, P. K. Geostatistics. Chapter 20 in: *Handbook of Hydrology*, 551 pp., D.R. Maidment, (Ed.). McGraw-Hill, NY, 1992.

Kohler, M. A., and L. H. Parmele. Generalized estimates of free-water evaporation, *Water Resources Research, 3(4)*: 997-1005, 1967.

Kovacs, G. Estimation of average areal evapotranspiration – proposal to modify Morton's model based on the complementary character of actual and potential evapotranspiration. *J. Hydrol.*, 95: 227-240, 1987.

LeDrew, E. F. A diagnostic examination of a complementary relationship between actual and potential evapotranspiration. *J. Appl. Meteorol.*, 18: 495-501, 1979.

Lemeur, R., and L. Zhang. Evaluation of three evapotranspiration models in terms of their applicability for an arid region. *J. Hydrol.*, 114: 395-411, 1990.

Lhomme, J. -P. A theoretical basis for the Priestley-Taylor coefficient. *Boundary Layer Meteorol.*, 82: 179-191, 1997.

McNaughton, K. G., and T. W. Spriggs. An evaluation of the Priestley and Taylor equation and the complementary relationship using results from a mixed-layer model of the convective boundary layer. *Estimation of areal evapotranspiration.* IAHS, Publ. No. 177: 89-104, 1989.

Mooty, W. S., and H. H. Jeffcoat. *Inventory of inter basin transfer of water in the eastern United States.* U.S. Geological Survey, open-file report 86-148, 1986.

Morton, F. I. Potential evaporation and river basin evaporation. *J. Hydraul. Div.*, ASCE, 91(HY6): 67-97, 1965.

Morton, F. I. Climatological estimates of evapotranspiration. *J. Hydraul. Div.*, ASCE, XX(HY3): 275-291, 1976.

Morton, F. I. Operational estimates of areal evapotranspiration and their significance to the science and practice of hydrology, *J. Hydrol.*, 66: 1-76, 1983.

Morton, F. I., F. Ricard, and S. Fogarasi. Operational estimates of areal evapotranspiration and lake evaporation – Program WREVAP, *National Hydrology Research Institute*, Paper No. 24, Ottawa, Canada, 75 pp., 1985.

Nash, J. E. Potential evaporation and "the complementary relationship". *J. Hydrol.*, 111: 1-7, 1989.

NREL. *User's Manual for National Solar Radiation Data Base (1961-1990)*. National Renewable Energy Laboratory, Golden, Colorado, U.S.A. 93 pp., 1992.

Parlange, M. B., and G. G. Katul. Estimation of the diurnal variation of potential evaporation from a wet bare soil surface. *J. Hydrol.*, 132: 71-89, 1992a.

Parlange, M. B., and G. G. Katul. An advection-aridity evaporation model. *Water Resour. Res.*, 28(1): 127-132, 1992b.

Penman, H. L. Natural evaporation from open water, bare soil and grass, *Proc. R. Soc. London, Ser. A.*, 193: 120-146, 1948.

Petsch, H. E. Jr. *Inventory of inter basin transfer of water in the western conterminous United States*. U.S. Geological Survey, open-file report 85-166, 1985.

Priestley, C. H .B., and R. J. Taylor. On the assessment of surface heat flux and evaporation using large-scale parameters, *Monthly Weather Review*, 100: 81-92, 1972.

Ramírez, J. A., and L. Claessens. Large scale water budgets for the United States, Hydrologic Science and Engineering Department, Colorado State University, Final Progress Report Cooperative Agreement No. 28-C2-618, Fort Collins, Colorado, U.S.A., 153 pp., 1994.

Sharma, T.C. An evaluation of evapotranspiration in tropical central Africa. *Hydrol. Sci. J.*, 33(2): 31-40, 1988.

Slack, J. R., and J. M. Landwehr. *Hydro-climatic data network (HCDN): A U.S. Geological Survey streamflow data set for the United States for the study of climate variations, 1874-1988*. U.S. Geologic Survey, open-file report 92-129, 1992.

Slatyer, R. O., and I. M. McIlroy. *Practical Microclimatology*, 310 pp., CSIRO, Melbourne, Australia, 1961.

Solley, W.B., C.F., Merk, and R.R. Pierce. *Estimated use of water in the United States in 1985*. U.S. Geological Survey, circular 1004. 82 pp., 1988.

Stewart, R. B., W. R. Rouse. A simple method for determining the evaporation from shallow lakes and ponds. *Water Resources Research.* 12, 623-628, 1976.

Stewart, R.B., W.R. Rouse. Substantiation of the Priestley and Taylor parameter $\alpha = 1.26$ for potential evaporation in high latitudes. *J. of Applied Meteorology.* 6, 649-650, 1977.

Tabios, G. Q., and J. D. Salas. A comparative analysis of techniques for spatial interpolation of precipitation. *Water Resour. Bull.*, 21(3): 365-380, 1985.

U. S. Geological Survey. Class A pan evaporation for period 1931—1960. *The National Atlas of the United States of America.* U.S. Geological Survey. Washington, D.C., 417 pp., 1970.

Van Bavel, C. H. M. Potential evaporation: the combination concept and its experimental verification, *Water Resour. Res.*, 2(3): 455-467.

Wallis, J. R., D. P. Lettenmaier, and E. F. Wood. A daily hydroclimatological data set for the continental United States, *Water Resources Research*, 27(7): 1657-1663, 1991.

Wright, J. L. New evapotranspiration crop coefficients. *J. Irrig. and Drain. Div.*, ASCE, 108(IR2): 57-74, 1982.

Table 1: Classification of selected basins by size.

Basin area (km^2)	# HUCs	# basins
< 5,000	75	72
5,000 – 10,000	50	33
10,000 – 20,000	68	20
20,000 – 40,000	64	10
40,000 – 100,000	39	3
> 100,000	55	1
Total	351	139

Table 2: Summary statistics for water balance closure errors.

Model \ Statistic		Mean [% prcp]	Median [% prcp]	Minimum [% prcp]	Maximum [% prcp]	St. Dev. [% prcp]	Skewness
CRAE (complete)		-2.35	-1.24	-43.13	24.87	7.69	-0.9908
AA	Validation*	8.56	12.23	-38.31	26.69	13.45	-1.6751
	Complete	7.92	10.55	-48.71	30.11	12.67	-1.7501
AA(1) (complete)		27.05	24.36	-16.47	74.21	18.98	0.5117
AA(2)	Calibration	6.17	6.91	-37.79	30.99	9.25	-1.1917
	Validation	7.93	8.21	-7.10	17.75	5.32	-1.0156
	Complete	6.76	7.38	-37.79	30.99	8.16	-1.3547
AA(2*)	Calibration	0.00	2.02	-49.55	25.35	10.51	-1.5358
	Validation	1.15	1.65	-19.59	12.16	6.66	-1.0886
	Complete	0.39	1.80	-49.55	25.35	9.37	-1.6049

* Refers to those sets of basins used to validate the AA(2) and AA(2*) models.

Figure 1: Schematic representation of the complementary relationship in regional evapotranspiration (assuming constant energy availability).

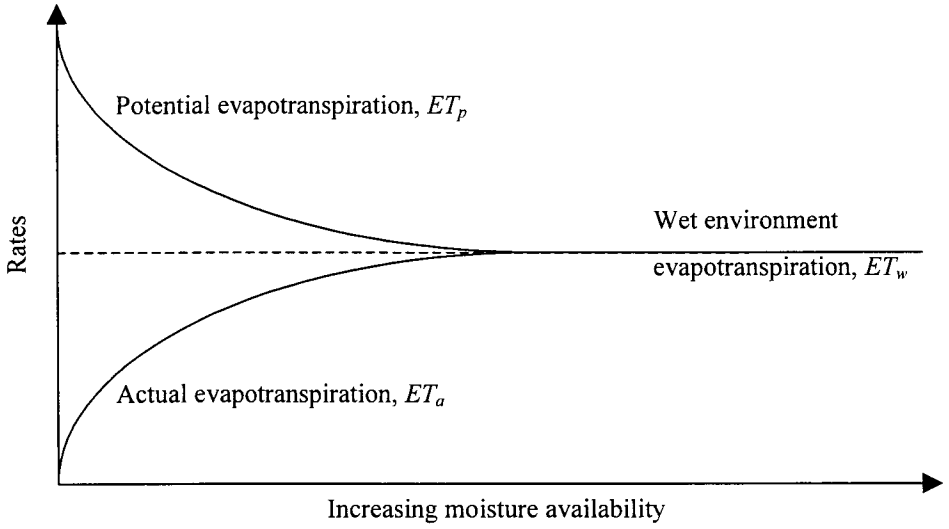

Figure 2a: Histogram of closure errors ε^{CRAE} and ε^{AA}.

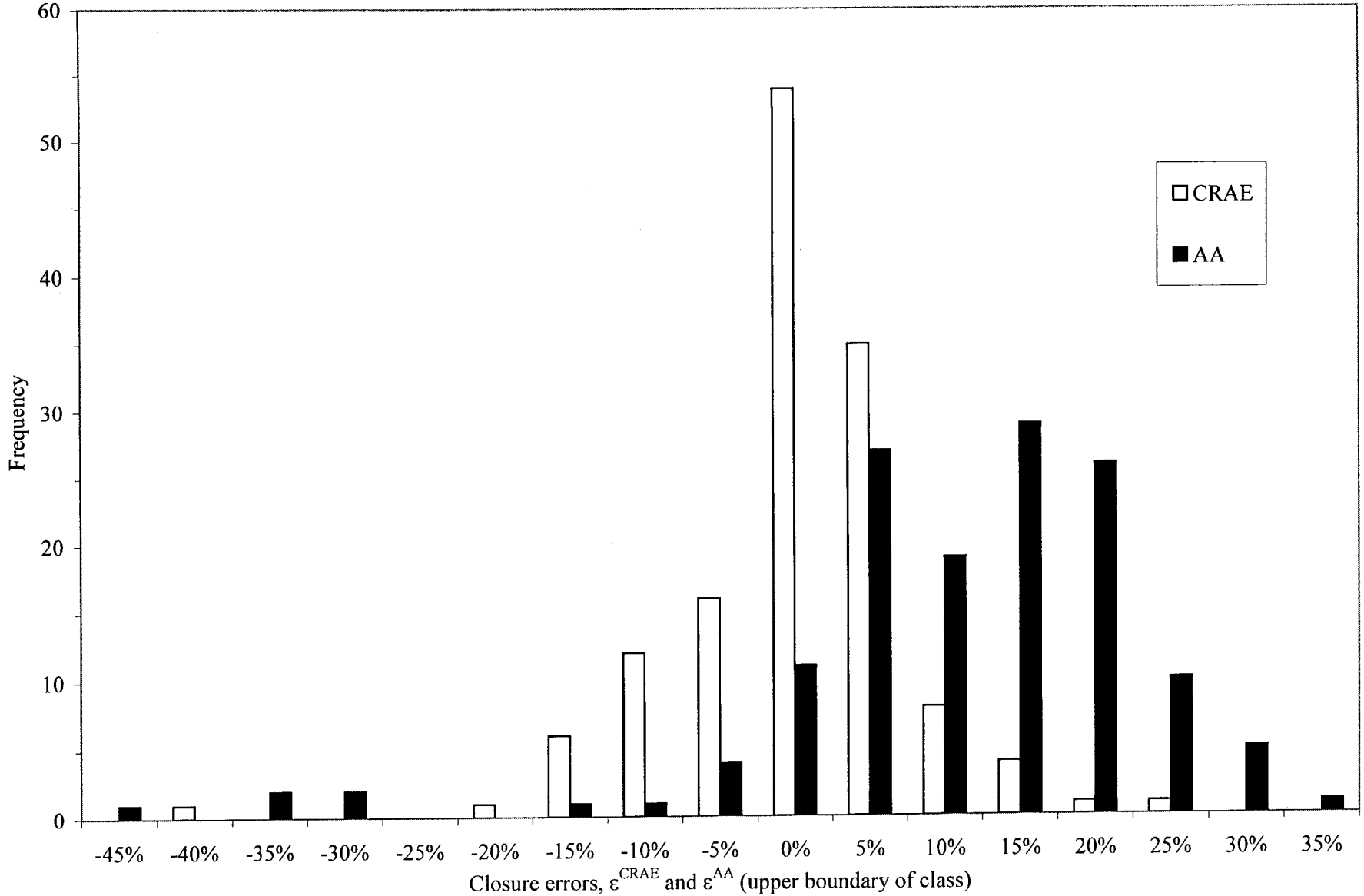

Figure 2b: Closure errors ε^{CRAE} and ε^{AA} versus mean annual basinwide wind speed.

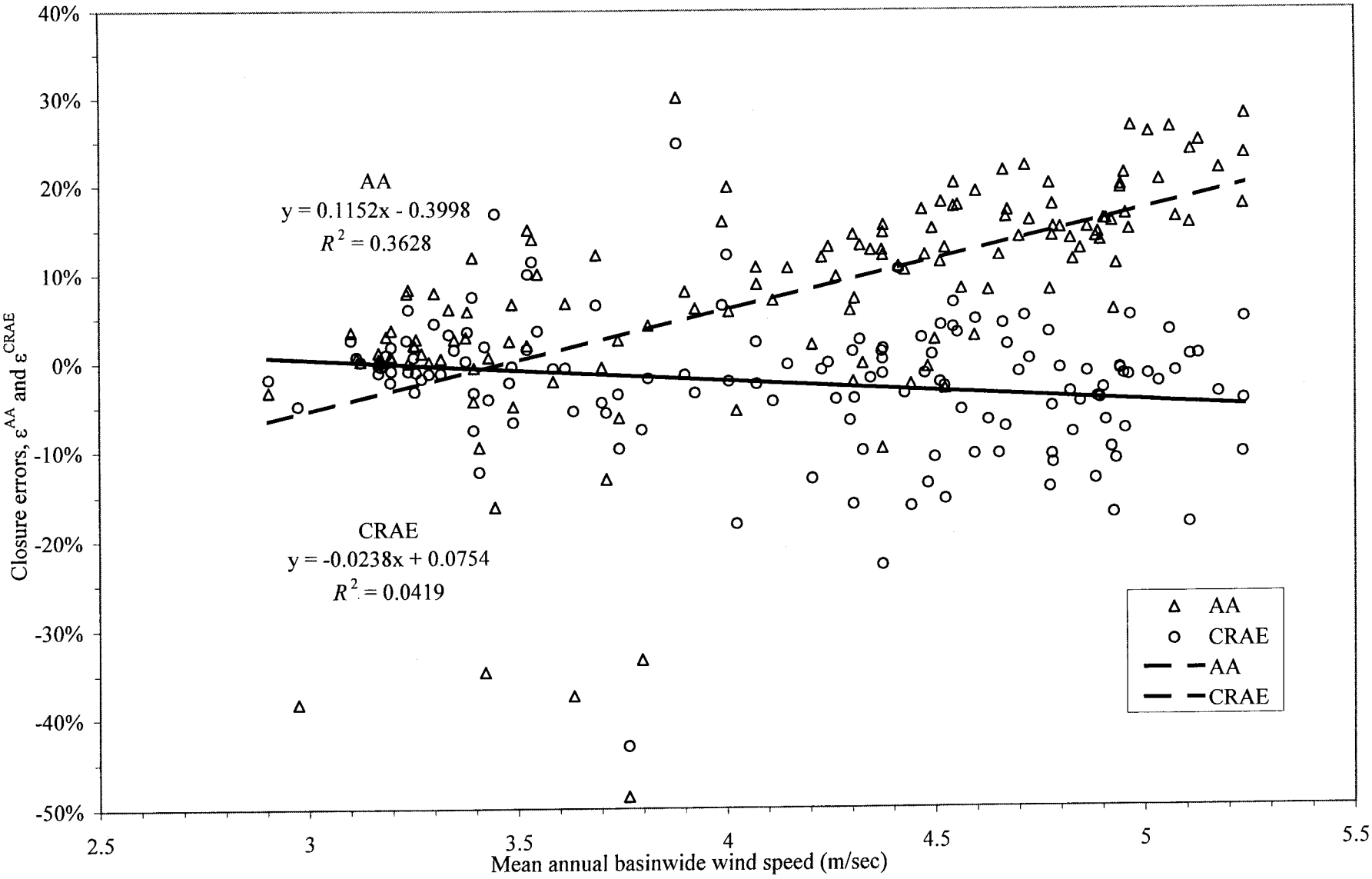

Figure 3: Example monthly $f(U_2)$ -U_2 relationship: August.

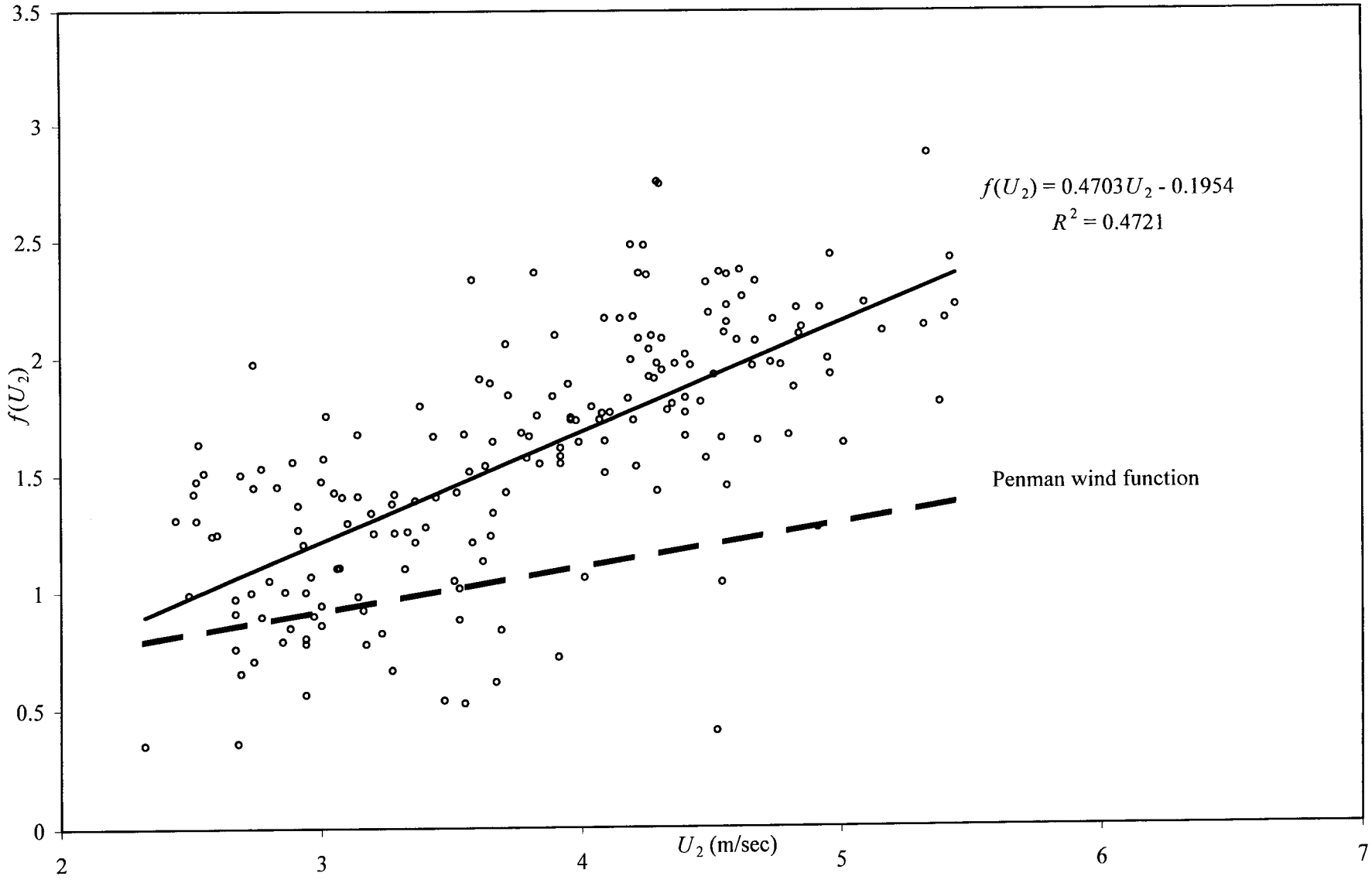

Figure 4a: Histogram of closure errors ε^{AA} and $\varepsilon^{AA(1)}$.

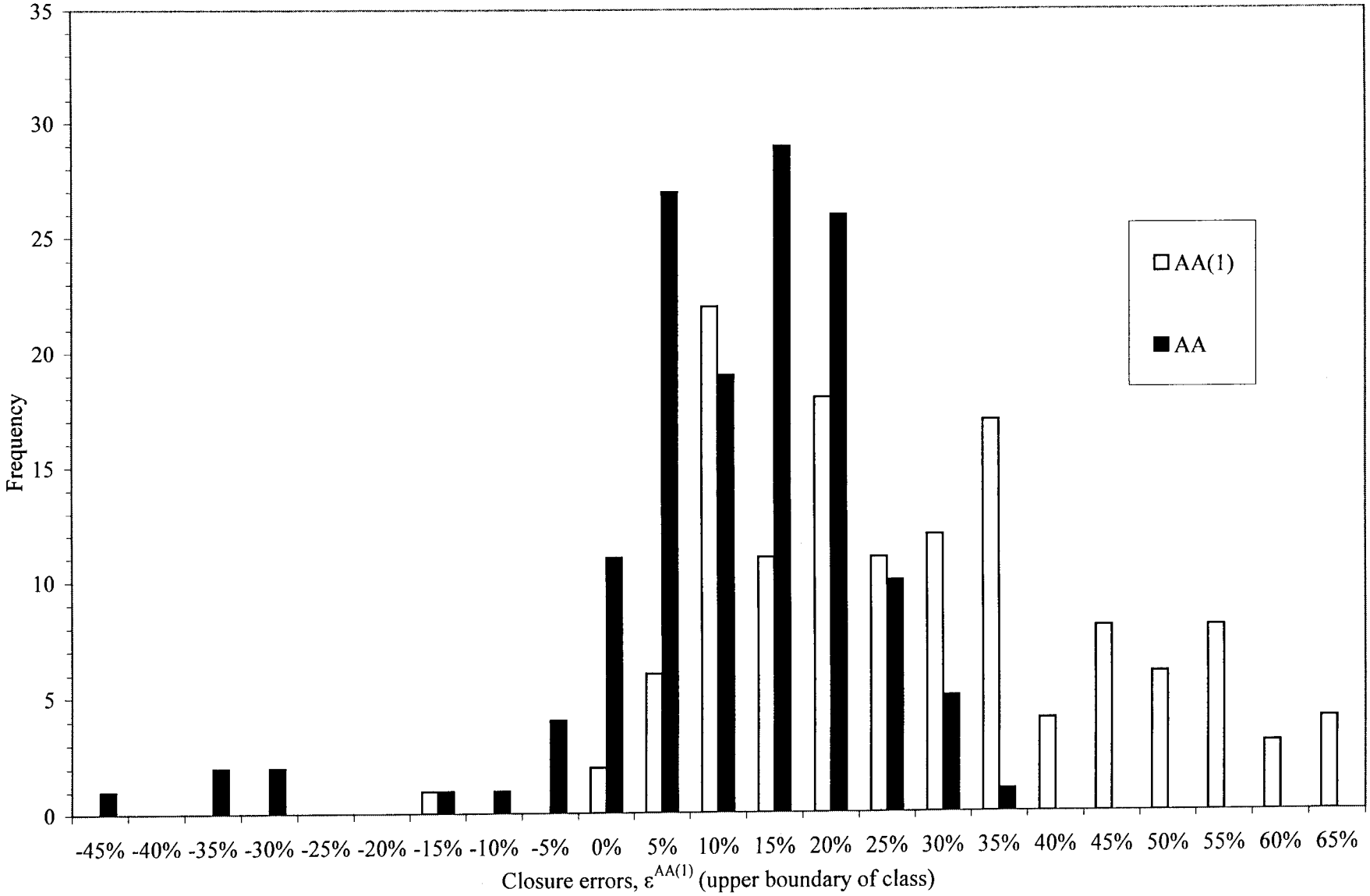

Figure 4b: Closure errors $\varepsilon^{AA(1)}$ versus mean annual basinwide wind speed.

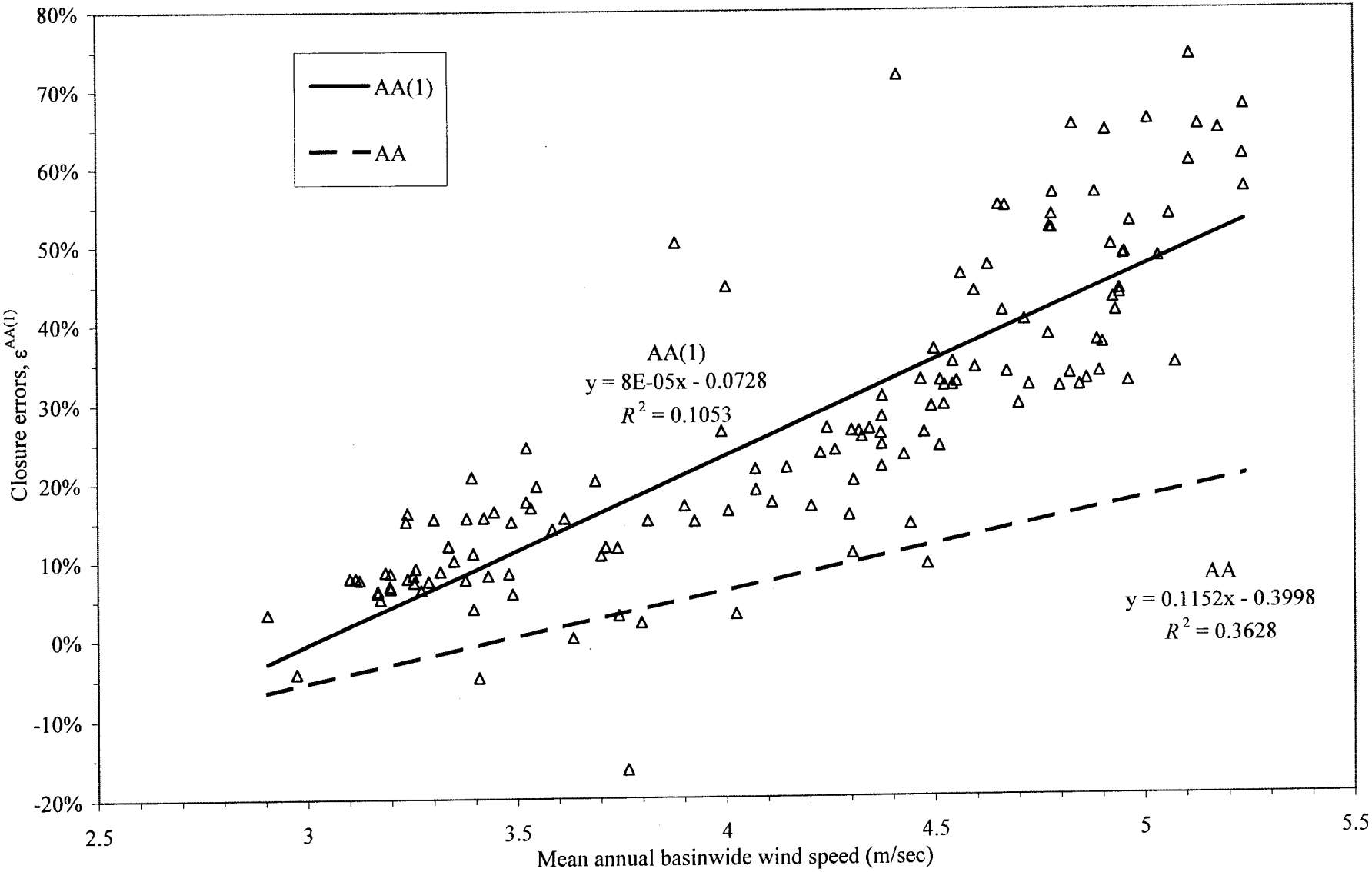

Figure 5a: Example of regional, seasonal $f(U_2)$ -U_2 relationships: Region 11.

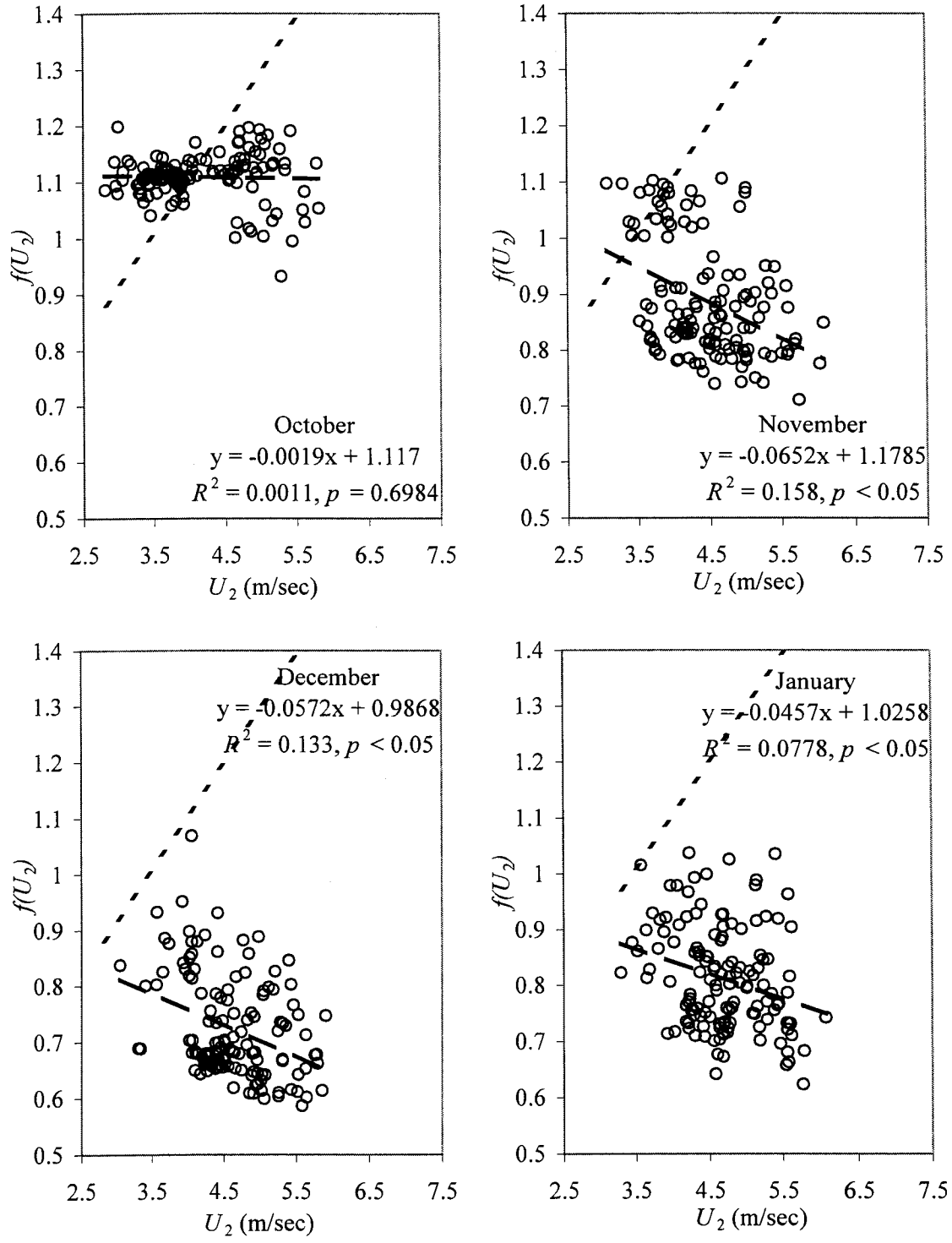

Figure 5a: Example of regional, seasonal $f(U_2)$ -U_2 relationships: Region 11.

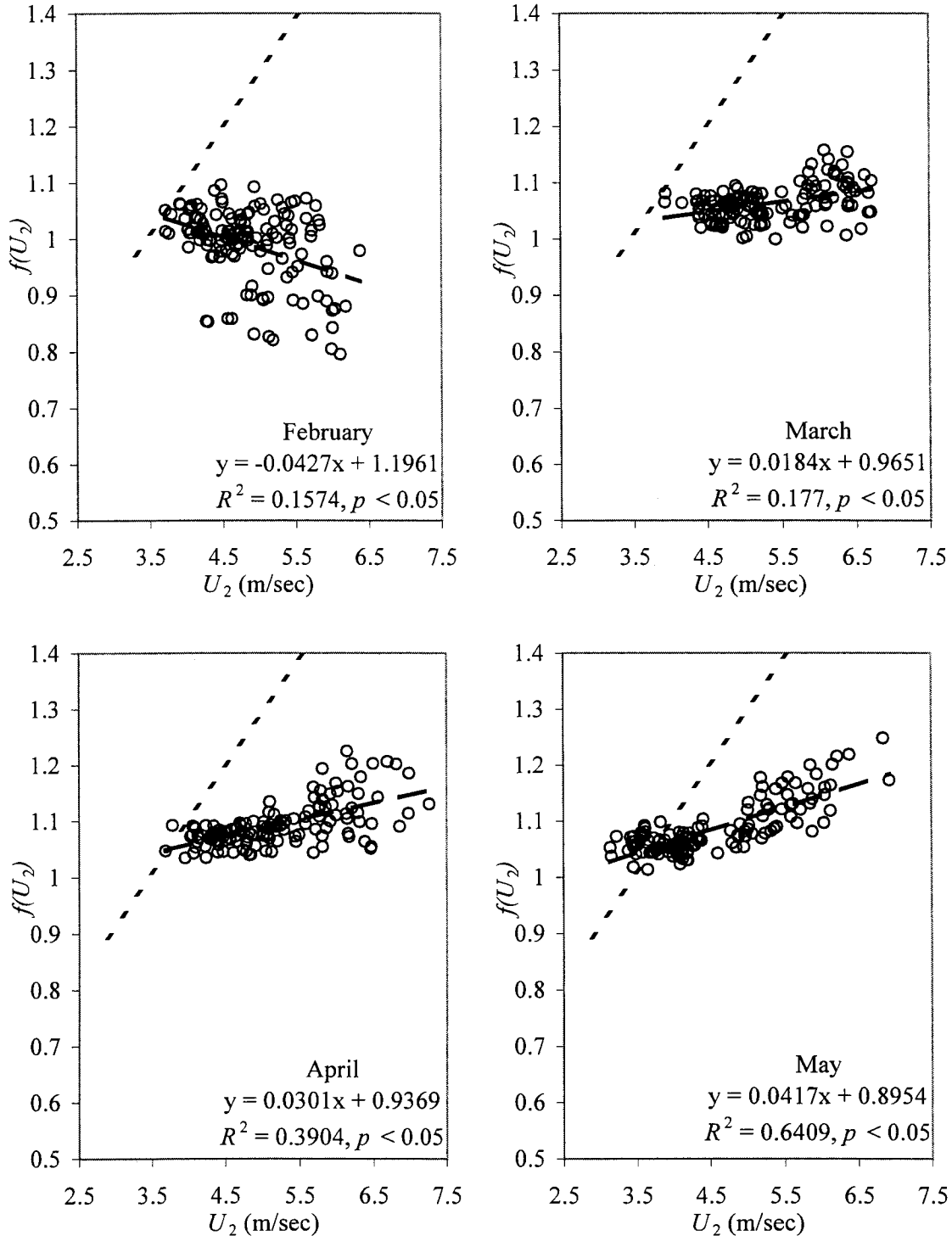

Figure 5a: Example of regional, seasonal $f(U_2)$ -U_2 relationships: Region 11.

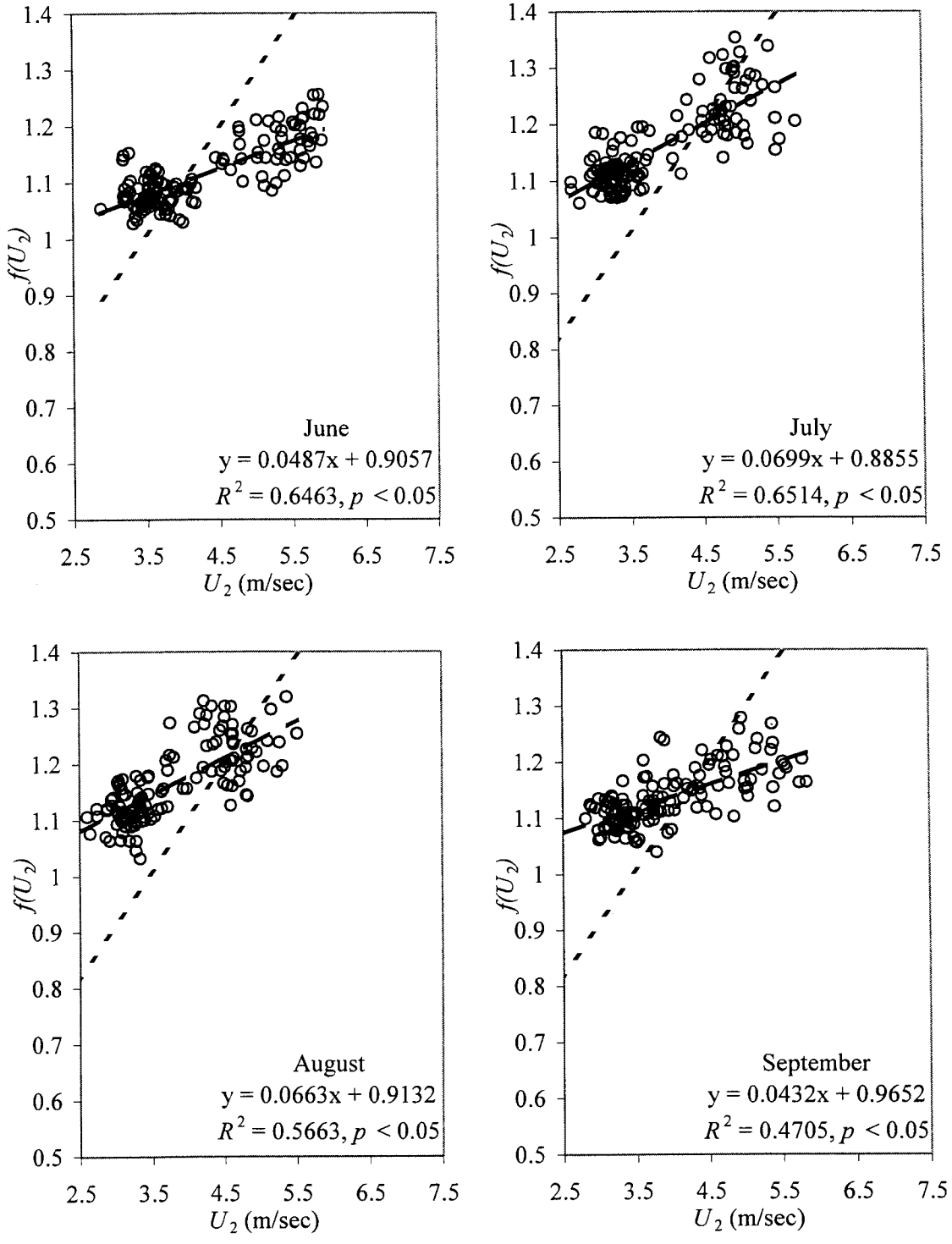

Figure 5b: Histogram of closure errors $\varepsilon^{AA(2)}$.

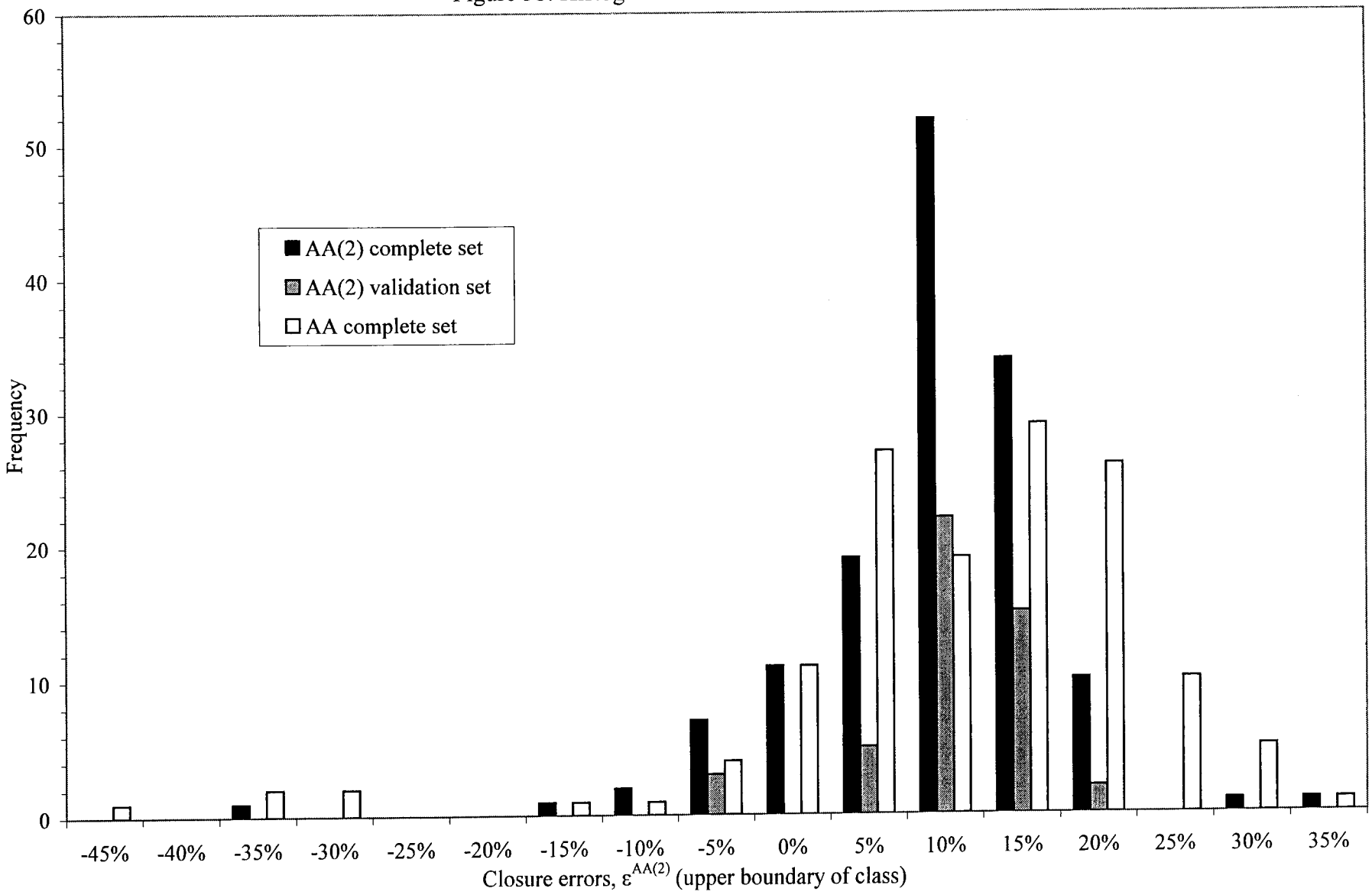

Figure 5c: Closure errors $\varepsilon^{AA(2)}$ versus mean annual basinwide wind speed.

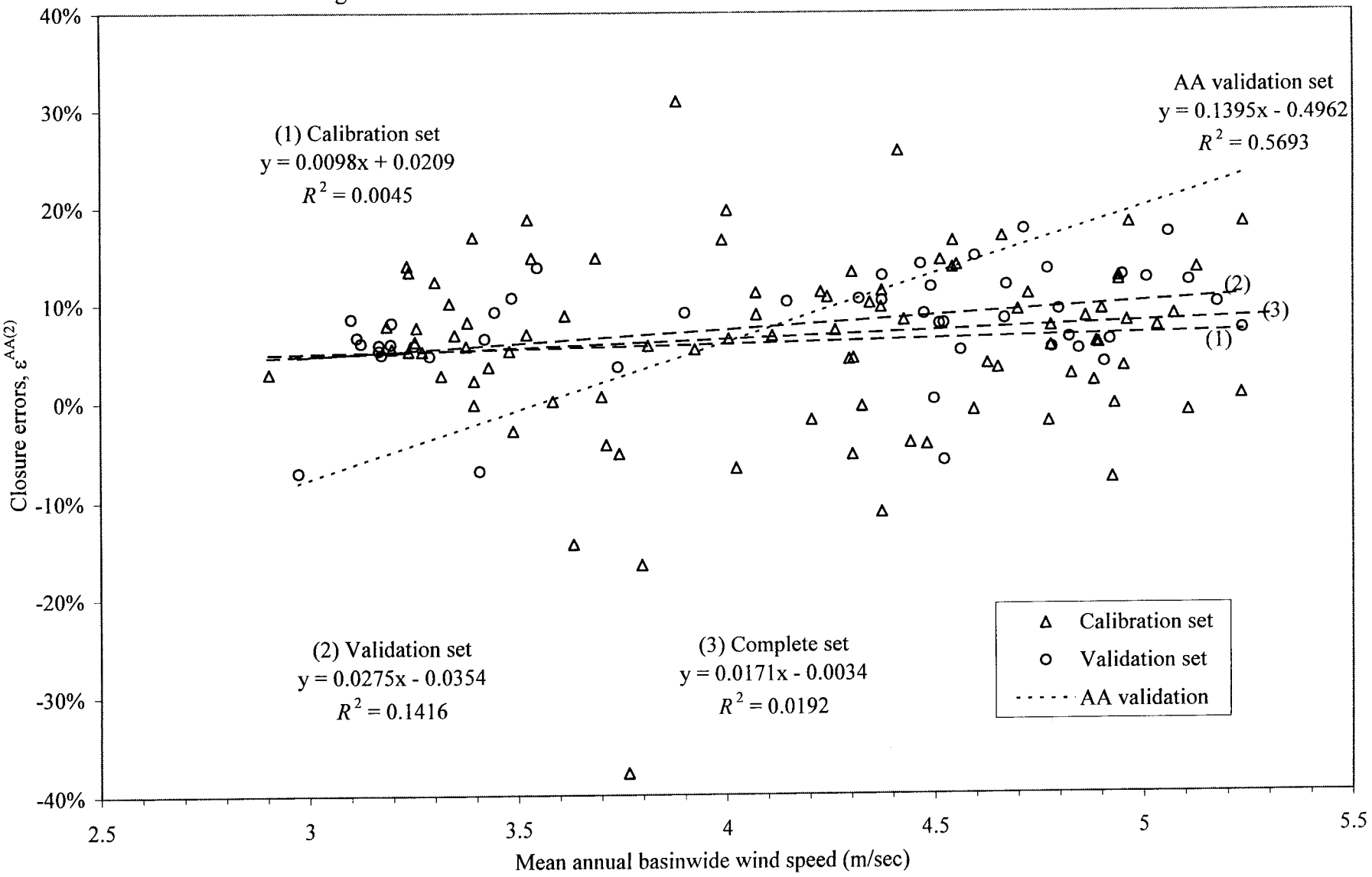

Figure 6: Mean closure errors $\varepsilon^{AA(2^*)}$ versus Priestley-Taylor coefficient trial values α.

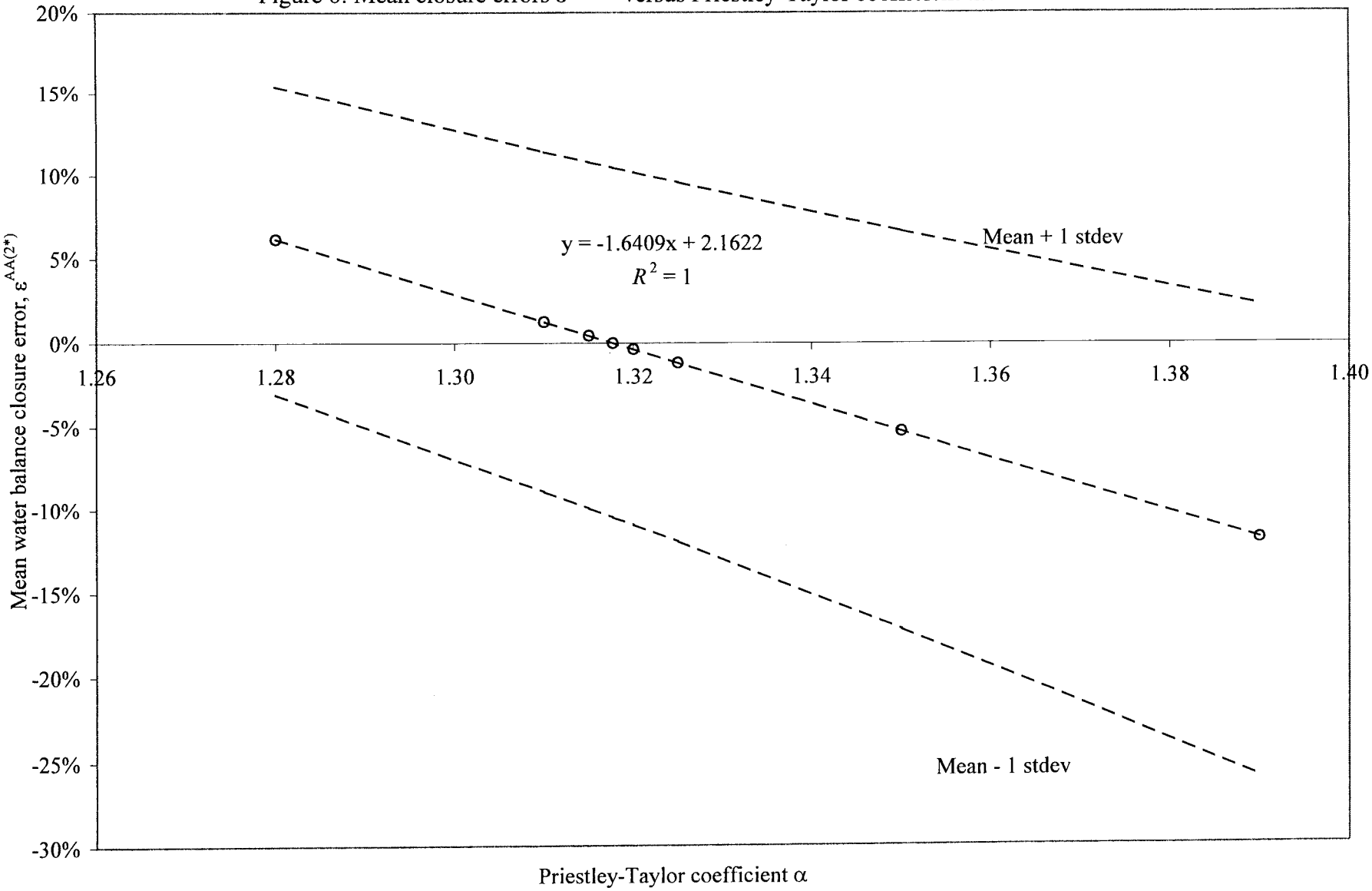

Figure 7a: Histogram of closure errors $\varepsilon^{AA(2^*)}$.

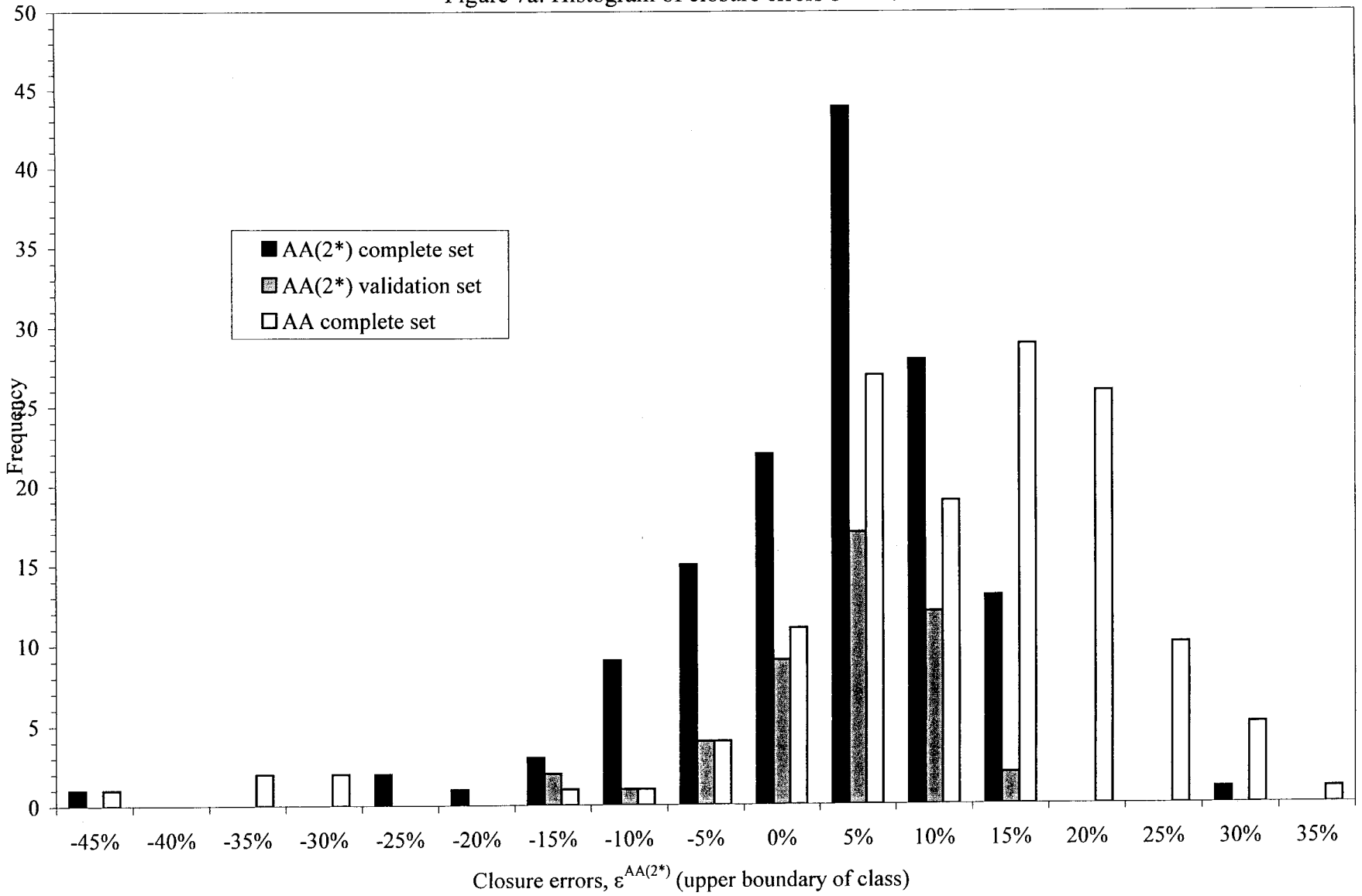

Figure 7b: Closure errors $\varepsilon^{AA(2^*)}$ versus mean annual basinwide wind speed.

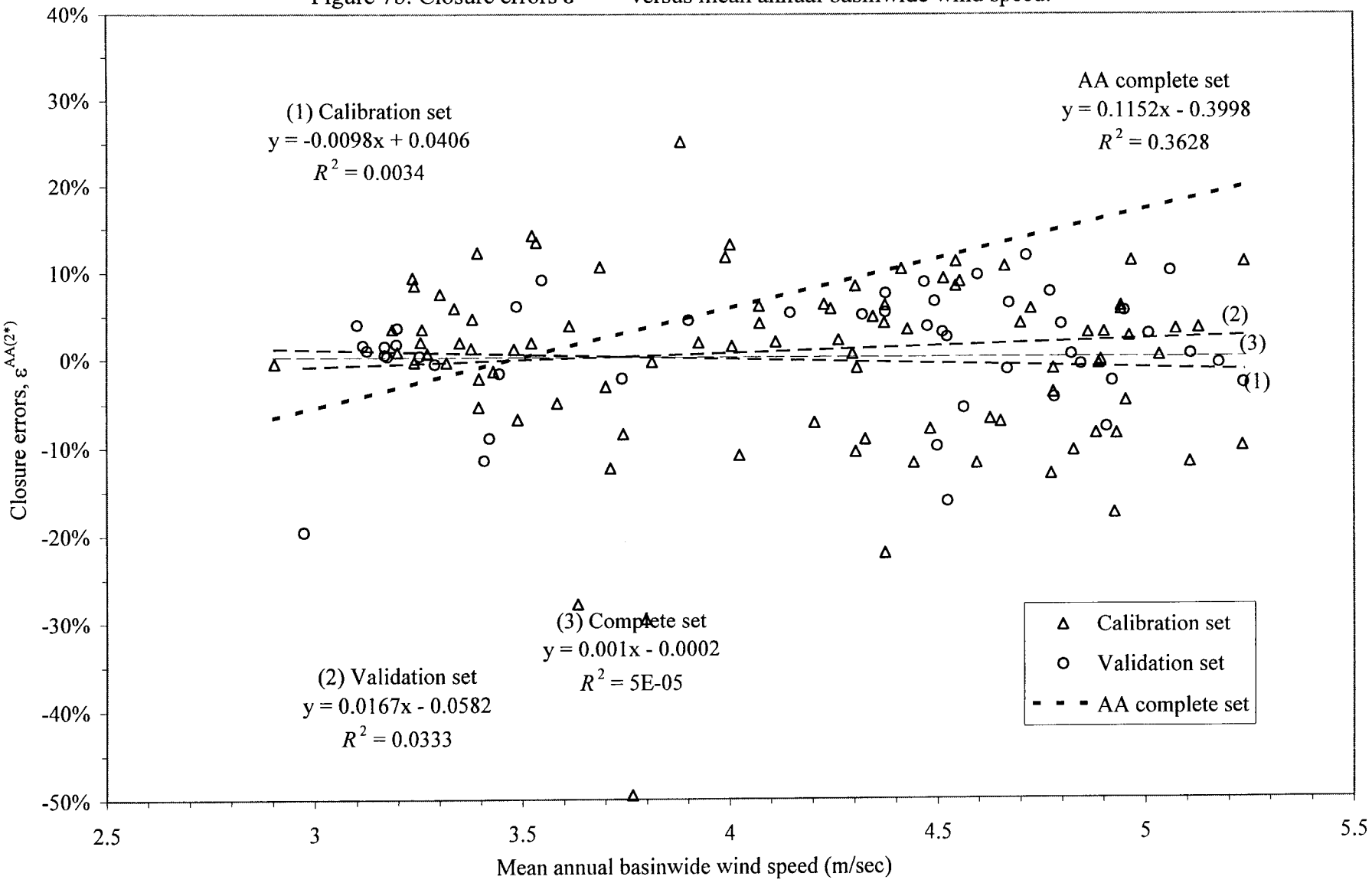

Figure 7c: Closure errors $\varepsilon^{AA(2^*)}$ versus mean annual basinwide precipitation.

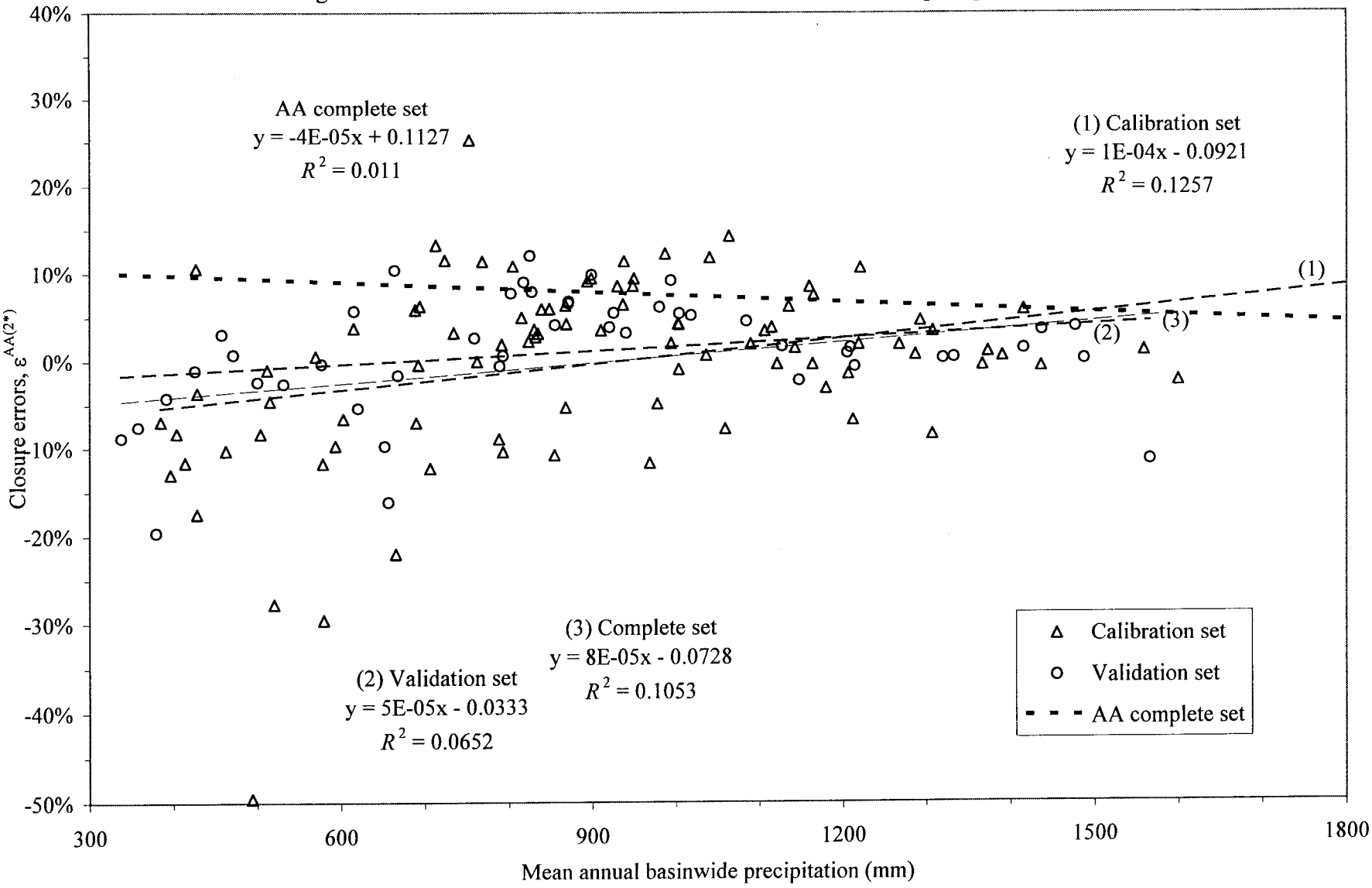

Figure 7d: Closure errors $\varepsilon^{AA(2^*)}$ versus mean annual basinwide ET_a*.